Computers & Operations Research 141 (2022) 105690

Contents lists available at ScienceDirect

Computers and Operations Research

journal homepage: www.elsevier.com/locate/cor

Fair allocation of personal protective equipment to health centers during early phases of a pandemic

Zehranaz Dönmez [a,*], Serkan Turhan [b], Özlem Karsu [a], Bahar Y. Kara [a], Oya Karaşan [a]

[a] Department of Industrial Engineering, Bilkent University, Ankara, Turkey
[b] Department of Management Sciences, University of Waterloo, Waterloo, Canada

ARTICLE INFO

Keywords:
Healthcare resource allocation
Personal protective equipment allocation
Pandemic
Fairness
Equity
COVID-19
Epsilon-constraint algorithm
Genetic algorithm

ABSTRACT

We consider the problem of allocating personal protective equipment, namely surgical and respiratory masks, to health centers under extremely limited supply. We formulate a multi-objective multi-period non-linear resource allocation model for this problem with the objectives of minimizing the number of infected health workers, the number of infected patients and minimizing a deprivation cost function defined over shortages. We solve the resulting problem using the ϵ-constraint algorithm so as to obtain the exact Pareto set. We also develop a customized genetic algorithm to obtain an approximate Pareto frontier in reasonable time for larger instances. We provide a comparative analysis of the exact and heuristic methods under various scenarios and give insights on how the suggested allocations outperform the ones obtained through a set of rule-of-thumb policies, policies that are implemented owing to their simplicity and ease-of-implementation. Our comparative analysis shows that as the circumstances get worse, the trade-off between the deprivation cost and the ratio of infections deepens and that the proposed heuristic algorithm gives very close solutions to the exact Pareto frontier, especially under pessimistic scenarios. We also observed that while some rule-of-thumb policies such as a last-in-first-receives type policy work well in terms of deprivation costs in optimistic scenarios, others like split policies perform well in terms of number of infections under neutral or pessimistic settings. While favoring one of the objectives, these policies typically fail to provide good solutions in terms of the other objective; hence if such policies are to be implemented the choice would depend on the problem characteristics and the priorities of the policy makers. Overall, the solutions obtained by the proposed methods imply that more complicated distribution schemes that are not induced by these policies would be needed for best results.

1. Introduction

Pandemics and epidemics are acknowledged among the most challenging biological natural disasters by the International Federation of Red Cross and Red Crescent Societies (2020). Before 2019, the most recent viral diseases are severe acute respiratory syndrome (SARS) and H1N1. Centers for Disease Control and Prevention (CDC) stated that 26 countries suffered from SARS epidemic, which resulted in more than 8000 infections and 770 deaths during 2003. (CDC, 2017). H1N1 flu virus emerged in 2009 and caused a worldwide pandemic. It is estimated that 151,700–575,400 people died due to H1N1 as stated by CDC (2019a). Most recently, at the end of 2019, COVID-19 virus was identified in Wuhan, China. On March 11, 2020, World Health Organization (WHO) declared pandemic for COVID-19 virus, which has killed more than 3.5 million people over the past year (WHO, 2020c).

According to a framework by WHO (2017), pandemics can be described by four phases based on a global risk assessment procedure: Inter-pandemic phase, alert phase, pandemic phase and transition phase. The inter-pandemic phase is the preparation phase between pandemics. If a virus is identified in humans for the first time, alert phase starts where a detailed capacity planning and risk assessment are required in both global and local levels. If the virus is globally spreading, pandemic phase starts. Alert phase and pandemic phase are response phases. As the global risk level reduces transition phase (recovery) takes place, where the process is evaluated. During a pandemic the main purposes of the policy makers are as follows: preventing the spread of the disease, monitoring, evaluating and preparing the health systems, planning the future actions for governments and other stakeholders and implementing the corresponding measures both at individual and social levels. Hierarchy of Controls is implemented to

* Corresponding author.
E-mail addresses: zehranaz.donmez@bilkent.edu.tr (Z. Dönmez), sturhan@uwaterloo.ca (S. Turhan), ozlemkarsu@bilkent.edu.tr (Ö. Karsu), bkara@bilkent.edu.tr (B.Y. Kara), karasan@bilkent.edu.tr (O. Karaşan).

https://doi.org/10.1016/j.cor.2021.105690
Received 6 September 2021; Received in revised form 21 December 2021; Accepted 21 December 2021
Available online 10 January 2022

diminish the spread of the disease as well as protecting the front-line workers such as health care personnel (CDC, 2015). Engineering controls such as vaccination and air-borne isolation rooms are more favorable than administrative controls and using protective equipment since they prevent the spread at the source level. When these controls are not applicable, protective equipment becomes a primary measure. Transmission precautions should be implemented in health centers based on the ways pathogens are transmitted between individuals. For an air-borne disease, precautions include providing masks to the patients as source control and protecting healthcare personnel with adequate equipment (CDC, 2016).

Distribution strategies for the necessary medical equipment should be analyzed in inter-pandemic phases as well as the response (alert and pandemic) phases (WHO, 2017). These distribution strategies are mostly applied for healthcare workers who are exposed to high risk of infection during Aerosol Generating Procedures (AGP) and should be equipped with Personal Protective Equipment (PPE). PPEs are wearable tools, which include masks, gloves, gown and face shields to prevent infection between individuals (CDC, 2020c). The term "mask" includes various types based on leakage and filtering qualities, re-usability and test requirements. Surgical masks are generally worn by the patients whereas healthcare personnel should be equipped with respirators. Although respirators can be categorized as filtering face-piece respirators, powered air-purifying respirators, elastomeric respirators, supplied-air respirators, self-contained breathing apparatus and combination respirators; N95 filtering face-piece respirators are recommended for healthcare settings by CDC and therefore used as a PPE for medical staff. (CDC, 2016, 2019b). Throughout the paper, the terms "respiratory mask" and "respirator" are used to refer to single use N95 filtering face-piece respirators.

During the pandemic phase, PPE shortages can be experienced at the highest rate due to rapidly rising demand. Therefore, defining and solving the PPE allocation problems for this phase is more crucial compared to other phases.

One of the aims of this paper is to define PPE distribution problem accurately. Choosing the most challenging phase in terms of resource allocation, the problem is modeled considering the main actions, known and uncertain parameters, and the limiting constraints resulting from the operational dynamics.

If the disease is an air-borne disease like COVID-19, PPEs are most effective when they are used alongside the social distancing measures. If such measures are difficult to implement, PPE usage becomes extremely important. For instance, medical procedures usually require close contact between health workers and patients therefore, the responsible organizations should provide both parties with the necessary PPE. Especially during AGP, health workers are exposed to high level of infection risk and they are more likely to infect other people. Given that protecting health workers is a public health issue (WHO, 2013), allocation and distribution strategies for health institutions should be determined beforehand and these strategies should be customized considering the dynamics of each phase.

Distribution strategy depends on the item's shelf life. If the item is for single use the inventory of institutions should be regularly replenished as the demand occurs frequently and limited supply is available each day. If the shelf life of the item is sufficiently long, PPEs can be distributed to institutions beforehand to be used later. In general, inadequate supply of PPEs are more of a limiting factor for stocking compared to shelf life. Especially for surgical masks, supply amounts are quite insufficient in the early phases of the pandemic. WHO (2020b) declared that the production capacities for surgical masks should be increased by 40% to meet the demand of 89 million/month. To tackle the scarcity of PPEs during early phases of a pandemic, various solutions are discussed including extended use (Zhu et al., 2014) and re-use of equipment after they are decontaminated (Bergman et al., 2012; Rowan and Laffey, 2020), improving production capacities and establishing distribution strategies (Patel et al., 2017) and contingency capacity strategies (CDC, 2020b). Equitable allocation strategies for PPEs as one of the most scarce resources during a pandemic, should be investigated considering this supply and demand imbalance (Binkley and Kemp, 2020).

A fair allocation of PPEs is crucial in terms of ethical guidelines as well (Emanuel et al., 2020). To this end, policies that would save most lives should be implemented and the ones who play a role in fighting the pandemic should be prioritized. Hence, healthcare workers should be equipped with proper PPEs and equity should be ensured among them. While total utility should be maximized to ensure efficiency, fairness should be established by providing similar level of service to institutions with similar needs (e.g. hospitals).

In this study, our aim is to establish a centralized fair and efficient allocation of surgical and respiratory masks to a set of hospitals given an extremely limited supply during the pandemic phase. Total number of infected workers and patients are tried to be minimized along with an inequity function on shortages. To this end, a novel multi-objective multi-period non-linear resource allocation model is formulated and optimally solved using ϵ-constraint algorithm. A customized genetic algorithm is proposed to obtain the approximate Pareto frontier. Additionally, rule-of-thumb policies are developed to be used by the decision makers and comparative analysis between these policies, heuristic and optimal solutions are provided. To the best of our knowledge such a resource allocation model has not been studied in the infectious disease literature. Our methodology includes not only constructing such a complex bi-objective non-linear model but also solving it to optimality for small-sized instances. Although our problem tackles a pandemic situation, the adopted methodology provides a great level of insight on how to approach such allocation problems from any similar field.

The rest of the paper is organized as follows. In Section 2, we review the related literature. The allocation problem is defined in Section 3. We introduce the non-linear bi-objective multi-period mathematical model in Section 4. The solution methodology is explained in Section 5. In Section 6, the problem is solved using the ϵ-constraint method, the customized genetic algorithm and the set of rule-of-thumb policies followed by the discussion of results. Finally, Section 7 provides concluding remarks and some future research directions.

2. Related literature

2.1. OR in infectious disease management

Pandemics and epidemics are studied in the literature mostly from two aspects: (i) modeling the disease spread, (ii) improving the preventive and treatment activities (slowing the disease spread) (Liu et al., 2020). For modeling the disease spread, mathematical models such as SIR (susceptible-infectious-recovered) type models are used frequently (Choewell et al., 2016; Lee et al., 2012). These models divide the population into subgroups, namely compartments, to model the transmission of the disease. Complex network models and agent-based models are also used in the literature. The interested reader can refer to Duan et al. (2015) for a detailed literature review for epidemiology progression models.

For slowing down the disease transmission, policy adjustments are made and logistics activities are improved to provide necessary medical resources and treatments. Operations Research (OR) plays a crucial role in controlling pandemics and epidemics by improving the logistics operations such as facility location (Lee et al., 2006, 2009; Büyüktahtakın et al., 2018; Yang et al., 2021; Li et al., 2021), vehicle routing (Gamchi et al., 2021), inventory management (Hashikura and Kizu, 2009; Adida et al., 2011; Paul and Venkateswaran, 2018) and resource allocation. Disease spread is also modeled through networks aiming to minimize the contamination (Ventresca and Aleman, 2014; Nandi and Medal, 2016). A literature survey is conducted by Dasaklis et al. (2012) for logistics operations during epidemics. Studies that concern resource allocation problems for infectious disease management are listed in

Table 1. It is observed that most of these studies focus on vaccination, drug supply chain and medical staff allocation whereas PPE allocation is mostly neglected. An exception is a recent paper by Göçmen (2020) studying PPE allocation problem with demand uncertainty. They tackled uncertainty using fuzzy parameters with a focus on routing while neglecting the effect of PPE allocation on the number of infections. Scenario analysis consists of various scenarios for demand levels and inventory capacities. Our study differs from that of Göçmen (2020) with consideration of levels for numerous parameters such as reproduction and infection rates, supply and demand as well as the effect of allocation decisions on infections of health care workers and outpatients. Rowan and Laffey (2020) recently studied policies to handle the shortage of PPE during COVID-19 such as reprocessing, however their focus is more on a conceptual perspective rather than constructing and solving the problem mathematically. Common resource allocation modeling approaches in infectious disease management are discussed by Brandeau (2005).

2.2. Equitable resource allocation in infectious disease management

Equity is an important concern when it comes to serving vulnerable groups of people in the context of disaster management. As a branch of this, infectious disease management should include fair allocation strategies to contribute public health respecting the ethical principles of humanitarian operations as stated by Sokat and Altay (2021) and Brandeau (2005). The concern for equity becomes even more pronounced considering the possible scarcity of items of need that should be delivered to populations such as preventive (PPE, vaccine etc.) and remedial (drugs, hospital beds, medical staff etc.) medical resources.

Prioritization of populations based on the infection and/or death risk level is one of the most used approaches in the OR literature while allocating resources in case of an epidemic/pandemic. Preventive approaches for the infectious diseases include prioritization based on risk levels of the populations (Kaplan and Pollack, 1998; Lasry et al., 2007) whereas treatment resources are allocated considering the severity of symptoms of the patients (Rico et al., 2007; Sun et al., 2014; Anparasan and Lejeune, 2019).

Ensuring a minimum service level for all populations (Anparasan and Lejeune, 2019) or maximizing the minimum service level provided to populations (Sun et al., 2014) are also well-known methods where the former can be seen as a variant of the latter. The difference is that the minimum is limited in a constraint if the former is utilized instead of being maximized in the objective function. Deviation between service levels (Yin and Büyüktahtakın, 2021) and Gini coefficient (Enayati and Özaltın, 2020) can also be used to ensure a balanced allocation. The definition of service level depends on the problem as well as the goals set while constructing the problem.

The last two methods are only considering service levels in terms of the allocation amounts if used alone. However, in the context of disaster management, shortage can cause human suffering which increases non-linearly with the waiting time. Therefore, taking the waiting time of populations for the items and/or services to be provided into account makes the problem definitions resemble the real life situations more closely. The concept of "Deprivation Cost Function" (DCF) introduced by Holguín-Veras et al. (2013) is defined as the economic value of the human suffering caused by a lack of access to a good or service and captures the effect of this time aspect of allocations as well as the amounts allocated on the resulting suffering of populations.

Although DCFs has drawn increasing attention in the field of humanitarian logistics and disaster managements as stated by Shao et al. (2020), there are not many researches focusing on infectious disease management while utilizing DCFs. Malmir and Zobel (2021) focus on allocation of medical resources such as hand sanitizers and PPE to affected areas while minimizing transportation cost, inventory holding cost, and deprivation cost in response to COVID-19. The focus of this work is more on the transportation modes ad logistic issues in a multi-echelon structure rather than estimating and preventing transmission of the disease.

The contributions of this study can be listed as follows:

- To the best of our knowledge, there is no study that focuses on PPE allocation in response to a pandemic in a strategical level considering the effect of the allocation decisions on the future demands. This study aims to fill this gap.
- As highlighted by Brandeau (2005), equity is an important objective while allocating the resources during pandemics, which is overlooked in the literature. By utilizing deprivation cost as an objective function, a fair allocation of limited resources to health institutions is established during a pandemic.
- Various critical objectives such as minimizing the number of infections and minimizing deprivation cost are applied in a multi-period setting.
- A disease transmission model is used where mask distribution policies iteratively affect the arriving infected population on future time periods.
- Our model takes into account the close-contact transmission probabilities during medical procedures apart from the transmission rate within the society under normal circumstances.
- A non-linear bi-objective multi-period multi-item mathematical model is developed and solved to optimality for small sized problems indicating various possible scenarios during a pandemic.
- For the cases where the multi-period allocation problem is challenging to solve to optimality, a customized fine-tuned genetic algorithm is developed.
- Bi-objective structure of the problem is handled with ϵ-constraint algorithm to observe the true Pareto and with a customized genetic algorithm to obtain the approximate Pareto frontiers.
- Different distribution policies, which are easier in application are constructed and analyzed with respect to the optimal and the heuristic solutions under pessimistic, optimistic and neutral scenarios reflecting different levels of severity that can be encountered in real life.
- The proposed method will help the policy makers to make more informed decisions by analyzing the consequences of various allocation options.

3. Problem setting and real life dynamics

This study focuses on a setting where a certain amount of single-use surgical and respiratory masks are distributed to hospitals in a city where aim is a fair allocation. Each day, all supply must be distributed and hospitals may hold inventory of masks to use later as shelf lives of these items are sufficiently long. It is assumed that the city population is divided into subgroups where each subgroup receives service from a single hospital. Therefore, population served by each hospital is known beforehand.

Identical outpatients with same demand (1 surgical mask per person) arrive at each hospital to receive daily services on each day and each hospital has a specific number of doctors to provide this service. Due to the pandemic, these patients may have COVID-19 virus for which they and doctors they may see should be equipped with PPE. It is assumed that no patient or doctor uses their own resources for protective equipment therefore, all entities demand proper masks from the hospital. It is assumed that administrative and engineering controls are identical for the set of hospitals for which only demand and supply levels differ. Each outpatient has exactly one appointment in a hospital and the doctors working at the same hospital have equal work load, i.e. number of outpatients for each doctor is the same within a hospital. Each patient demands 1 surgical mask and demand of each doctor depends on the usage duration of PPEs and length of the shift, which is

Table 1
Literature review for resource allocation models for infectious diseases.

Reference	Resource type	Objective	Solution method	Multi-objective	Multi-period	Fairness
Kaplan and Pollack (1998)	Budget	Number of infections	Non-linear dynamic programming	–	–	+
Zaric and Brandeau (2002)	Budget	Number of infections or number of QALY's	Heuristic algorithm	–	+	–
Rico et al. (2007)	Medical staff	Number of patients in queue Patient flow	Simulation	+	–	+
Lasry et al. (2007)	Funds	Number of infections	Multi-level resource allocation model	–	–	+
Sun et al. (2009)	Medicine	Number of infections	Game theoretical approach	–	+	–
Koyuncu and Erol (2010)	Medicine Hospital beds Ventilators	Number of infections Number of deaths Number of morbidity days	Hierarchical multi-objective optimization	+	–	–
Tanner and Ntaimo (2010)	Vaccine	Vaccine coverage	Branch & cut algorithm	–	–	–
Araz et al. (2012)	Vaccine	Waiting time for vaccination Number of expected cases averted	Simulation	+	+	–
Teytelman and Larson (2013)	Vaccine	Number of infections	A heuristic algorithm	–	+	–
Ren et al. (2013)	Vaccine	Number of deaths	A heuristic algorithm	–	+	–
Liu and Liang (2013)	Medical resources	Total cost	A heuristic algorithm	–	+	–
Yarmand et al. (2014)	Vaccine	Vaccination cost	A heuristic algorithm	–	+	–
Sun et al. (2014)	Medical staff	The total travel distance The maximum travel distance	Linear programming	+	+	+
Chen et al. (2015)	Vaccine Medicine	Number of deaths	Barrier approach with Lagrangian relaxation	–	+	–
Liu et al. (2015)	Medical resource	Total logistics cost	A heuristic algorithm	–	+	–
Rachaniotis et al. (2017)	Medical staff	Number of infections	Heuristic algorithm	–	+	–
Long et al. (2018)	Hospital beds	Number of infections	Two-stage epidemic model Policy analysis	–	+	–
Anparasan and Lejeune (2019)	Medical staff Ambulance	Patient flow	Linear programming with hierarchical constraints and valid inequalities	–	–	+
Enayati and Özaltın (2020)	Vaccine	Amount of vaccine used	Optimization based on discretization with multi-parametric disaggregation	–	–	+
Göçmen (2020)	PPE	Total cost	Inventory routing problem with fuzzy parameters	–	+	–
Malmir and Zobel (2021)	Relief items	Transportation cost Deprivation cost	Non-linear programming	+	+	+
Yin and Büyüktahtakın (2021)	Treatment centers and resources	Number of infections Number and deaths	Multi-Stage stochastic programming	–	+	+
Yang et al. (2021)	Vaccine	Total facility and transportation cost	A sequential disaggregation and merging algorithm	–	–	–
Li et al. (2021)	Vaccine stations and medical staff	Average distance, number of facilities, total cost	Two-stage heuristic algorithm	+	–	–
Santini (2021)	Swap tests and reagent	The total and the ending inventory of swaps	Hierarchical integer programming	+	+	–
This study	PPE	Number of infections Deprivation cost	Non-linear programming Genetic algorithm Policy analysis	+	+	+

8 h. The maximum recommended wearing duration is 4 h according to WHO (2020a). Hence, it is supposed that each unit of supplies consists of 2 respirators.

This paper concerns only medical procedures that require close contact between the patient and the doctor and usage of protective equipment is possible for both parties (unlike dental and oral procedures). During such procedures, due to impossibility of distancing, mask usage is crucial and probability of transmission differs from the normal spreading behavior of the disease. Such medical procedures require respirator usage for doctors and patients should wear surgical masks (CDC, 2016). A patient who has COVID-19 virus may infect health workers depending on whether they and workers are equipped with mask or not. When structuring the mathematical model, for simplicity, it is assumed that an individual starts transmitting the disease as soon as they are infected, i.e. the time between infection and infectiousness is zero. The extension for the more general case where there is an incubation period is relatively straightforward. Moreover, an infected doctor may cause infection to other patients similarly depending on PPE use. In each appointment, one of the four cases occurs: both parties wear corresponding masks, none wears mask, only patient wears surgical mask or only doctor wears respirator. Overall transmission probability is calculated considering the probability of these cases.

Note that due to the disease spreading, increase in the number of currently infected patients causes an increase in the probability of infection in the patients arriving in the upcoming periods. Therefore, aim of this study is to mitigate the effect of the mask distribution policy of each period on demand levels of upcoming periods. This effect is measured in terms of the number of patients and doctors infected during appointments and the resulting increase in the ratio of infected patients in future periods. It is assumed that due to daily screen tests for health care workers, infected doctors are identified with 100% accuracy and quarantined each day. Therefore they do not contribute to the disease spreading outside of the appointments. Moreover, doctors are

Table 2
Parameters and decision variables of the mathematical model.

Parameters		*Decision variables*	
S_j^t	Amount of supplies of mask type j for period t	$X_{h,j}^t$	Amount of supply for mask type j allocated to hospital h on period t
$W_{h,1}^t$	Number of outpatients arriving on period t in hospital h	$Y_{h,t}$	Ratio of infected doctors at the end of period t in hospital h
$W_{h,2}^t$	Number of doctors at the beginning of period t in hospital h	$\alpha_{h,t}$	Ratio of infected individuals in the environment of hospital h at the beginning of period t
R	Reproduction rate	$Z_{h,t}$	Ratio of number of primary infections in period t in hospital h to the daily number of outpatients
Pop_h	Size of the population for which hospital h provides service	$I_{h,j}^t$	Inventory of mask type j in hospital h at the end of period t
β	Outward infection rate without mask	$U_{h,j}^t$	Shortage for mask type j in hospital h at the end of period t
β_j	Outward infection rate with mask type j	$DC_{h,j}^t$	Deprivation cost of hospital h on period t due to shortage on mask type j
θ	Inward infection rate without mask	*Auxiliary variables*	
θ_j	Inward infection rate of mask type j	$P_{h,t}^1$	Infection probability during an appointment in hospital h in period t due to an infected patient
$\alpha_{h,1}$	Ratio of infected arriving patients to hospital h at the beginning	$P_{h,t}^2$	Infection probability during an appointment in hospital h in period t due to an infected doctor
δ	Service level threshold for deprivation	$SL_{h,j}^t$	$\begin{cases} 1, & \text{If service level of hospital } h \text{ for mask type } j \\ & \text{is under the threshold at period } t \\ 0, & \text{otherwise} \end{cases}$

assumed to be uninfected at the beginning of each day since infected doctors are replaced with uninfected ones.

Due to the scarcity of supply, hospitals are likely to experience shortage during the planning horizon, which causes deprivation. Duration of this deprivation is as crucial as the amount deprived. Therefore, a deprivation cost function which measures both of these aspects of shortage is considered.

The aim is to provide corresponding masks (surgical masks for patients, respirators for doctors) to a set of hospitals so that number of infected health workers, number of infected patients and deprivation costs of hospitals are minimized considering a limited supply.

4. Mathematical model

A multi-objective multi-period non-linear programming model is developed which takes the number of doctors in each hospital, number of outpatients arriving each day, probability of infection with/without each mask type and disease spreading rate as input parameters. Outputs are the distributed amounts, inventory and shortage amounts for each mask type for each hospital at the end of each period. Our aim is to determine good mask allocation strategies so as to avoid the negative effect of sub optimal (unbalanced) allocations to the disease prevalence. To that end, we define infection probability for each hospital as a function of the number of masks distributed, ratio of infected doctors and infected patients and find the expected ratio of virus-carrier arriving patients depending on the number of previously infected patients. Given that the set of hospitals is H, the set of discrete time periods is T and the set of mask types are J where $|J| = 2$ (the first type of mask is surgical mask, while the second one is respirator); parameters and decision variables are given in Table 2.

Ratio of infectious individuals to the population for each hospital at the beginning is known whereas this ratio for next periods is recursively calculated depending on the infections during appointments and the proposed mask allocation.

There are four situations that can happen during appointments and probability of infection during an appointment depends on this as well as the infected side since inward and outward infection rates of surgical mask and respirator are quite different, as detailed in Table 3. For instance, let us consider the case where only patient wears surgical mask. If doctor is a carrier, patient is highly likely to be infected as inward protection of surgical masks is poor. On the other hand, if the patient is the carrier doctor is less likely to be infected due to adequate outward protection of the mask. Based on this, two infection rates are defined: infection rate due to an infected patient ($P_{h,t}^1$) and infection rate due to an infected doctor ($P_{h,t}^2$). These probabilities depend on the PPE demand satisfaction, hence they differ for each hospital h and each

Table 3
Possible cases for an appointment.

Possible cases	Probability of occurring	$P_{h,t}^1$	$P_{h,t}^2$
Both wearing mask	$\left(1-\frac{U_{h,1}^t}{W_{h,1}^t}\right)\left(1-\frac{U_{h,2}^t}{W_{h,2}^t}\right)$	$\beta_1\theta_2$	$\theta_1\beta_2$
None wearing mask	$\frac{U_{h,1}^t}{W_{h,1}^t}\frac{U_{h,2}^t}{W_{h,2}^t}$	$\beta\theta$	$\theta\beta$
Only patient wearing surgical mask	$\left(1-\frac{U_{h,1}^t}{W_{h,1}^t}\right)\frac{U_{h,2}^t}{W_{h,2}^t}$	$\beta_1\theta$	$\theta_1\beta$
Only doctor wearing respirator	$\frac{U_{h,1}^t}{W_{h,1}^t}\left(1-\frac{U_{h,2}^t}{W_{h,2}^t}\right)$	$\beta\theta_2$	$\theta\beta_2$

time period t (again, consider the case where only patient wears the proper mask). In hospital h, $U_{h,1}^t$ is the number of patients who are not provided a surgical mask in period t. Since the total number of visiting patients is $W_{h,1}^t$, probability of the patient having a surgical mask is $1-\frac{U_{h,1}^t}{W_{h,1}^t}$. Similarly, probability of the doctor not wearing a respirator is calculated as $\frac{U_{h,2}^t}{W_{h,2}^t}$. Moreover, probability of the scenario where only the patient is equipped with PPE is the multiplication of these two probabilities $\left(1-\frac{U_{h,1}^t}{W_{h,1}^t}\right)\frac{U_{h,2}^t}{W_{h,2}^t}$. In such a case (if the patient is the virus-carrier side of the appointment) the important parameters are the outward infection rate of the surgical mask (β_1) and the inward protection rate without any mask (θ) to calculate the probability of the doctor getting infected during the appointment. In Table 3, infection rates for possible cases and the corresponding probabilities are generated similarly. Moreover expected transmission probability is calculated by taking the weighted sum of these transmission rates.

There are 3 main iterative calculations in our approach: Calculating the ratio of infected doctors (Y), ratio of primary infections (Z) and ratio of infected individuals in the population of each hospital (α). Primary infection is defined as the number of infected patients during hospital appointments resulting from the mask allocation strategy in each time period. Since each doctor and patient get infected with a probability and multiplication with a probability cannot preserve integrality, infection cases are calculated as ratios of infected individuals to total number of individuals. Therefore, output variables Z, Y, α are continuous variables instead of integers.

Assuming that the daily workload of doctors are equal, each doctor in hospital h sees $\frac{W_{h,1}^t}{W_{h,2}^t}$ patients on day t. Consider the case for a single doctor who is uninfected and has $\frac{W_{h,1}^t}{W_{h,2}^t}$ appointments. Let p' be the probability of doctor getting infected during an appointment. We consider each appointment as a Bernoulli trial with success probability

$1-p'$ (Tuckwell and Williams, 2007). Since the number of patients per doctor may not be an integer, number of trials is taken as $\left\lceil \frac{W^t_{h,1}}{W^t_{h,2}} \right\rceil$. For the doctor to stay uninfected at the end of the day the outcome of all $\left\lceil \frac{W^t_{h,1}}{W^t_{h,2}} \right\rceil$ trials should be success.

Assuming that the trials are independent, the number of successes follows a Binomial distribution and it being $\left\lceil \frac{W^t_{h,1}}{W^t_{h,2}} \right\rceil$ has a probability of $(1-p')^{\left\lceil \frac{W^t_{h,1}}{W^t_{h,2}} \right\rceil}$. The expected number of doctors infected in day t in hospital h is given as $W^t_{h,2} \times (1-(1-p')^{\left\lceil \frac{W^t_{h,1}}{W^t_{h,2}} \right\rceil})$.

Correspondingly, ratio of infected doctors to the total number of doctors is given by Eq. (1).

$$Y_{h,t} = \frac{W^t_{h,2} \times (1-(1-p')^{\left\lceil \frac{W^t_{h,1}}{W^t_{h,2}} \right\rceil})}{W^t_{h,2}} = 1-(1-p')^{\left\lceil \frac{W^t_{h,1}}{W^t_{h,2}} \right\rceil} \tag{1}$$

Here, p' is the joint probability of two independent events: a patient being infected and transmission occurring during appointment due to this infected patient. As explained earlier, transmission probability in such a case is denoted as $P^1_{h,t}$. Assuming that the infected individuals in the population have equal probability of visiting the hospital on each day, ratio of infected individuals in the environment of hospital h in period t, $\alpha_{h,t}$, can be interpreted as the probability of an arriving patient being infected. Therefore, Eq. (2) gives the expected ratio of doctors infected on day t in hospital h.

$$Y_{h,t} = 1-(1-P^1_{h,t}\alpha_{h,t})^{\left\lceil \frac{W^t_{h,1}}{W^t_{h,2}} \right\rceil} \tag{2}$$

There are two types of arriving patients: infected and uninfected ones. Recall that primary infection is defined as the number of outpatients that are uninfected at the time of arrival and become infected at the time of leaving. Assuming that the infected individuals in the population have equal probability of visiting the hospital on each day, number of infected patient is $\alpha_{h,t}W^t_{h,1}$ for hospital h and period t and consequently number of uninfected arriving patients is $(1-\alpha_{h,t})W^t_{h,1}$ Supposing that the probability of infection for a patient is denoted by $\bar{p}$, an appointment is a Bernoulli trial with success probability $1-\bar{p}$ for an uninfected patient. For an infected arriving patient the success probability is 0.

Hence the expected number of primary infections would be $(1-\alpha_{h,t})W^t_{h,1}\bar{p}$. Corresponding ratio of primary infections for hospital h and period t is given in Eq. (3).

$$Z_{h,t} = \frac{(1-\alpha_{h,t})W^t_{h,1}\bar{p}}{W^t_{h,1}} = (1-\alpha_{h,t})\bar{p} \tag{3}$$

Note that the probability $\bar{p}$ can be written as the multiplication of probability of a doctor begin infected ($Y_{h,t}$) and transmission probability during an appointment due to an infected doctor ($P^2_{h,t}$) similar to p'. Based on this, Eq. (3) can be rewritten as Eq. (4).

$$Z_{h,t} = (1-\alpha_{h,t})(Y_{h,t}P^2_{h,t}) \tag{4}$$

The calculated ratio of primary infections for a period affects the infection ratio of population and consequently, the ratio of infected arriving patients on the next periods based on a disease spreading rate. This rate is defined as reproduction number R, which is the average number of secondary cases generated by a primary infectious individual (Choewell et al., 2016). That is to say that m infected individuals cause $R \times m$ individuals to be infected during the period they are infectious which is 10 days on average for persons with mild to moderate COVID-19 according to CDC (2020a). Therefore we simply assume that m infectious individuals transmit the disease to $R \times \frac{m}{10}$ people each day.

The system starts with a given ratio of infected patients who visit the hospitals at the beginning of the first period, $\alpha_{h,1}$. At the end of each period t, $Z_{h,t}W^t_{h,1}$ new cases arise due to hospital appointments (primary infections). Secondary cases due to primary infections on past days is already included as $\frac{(\alpha_{h,t-1})R}{10}$. While calculating α for the beginning of the next day, ratio of already infected individuals, $\alpha_{h,t-1}$, should be added as well. Since we investigate the initial phase in which there is scarcity, our planning horizon is shorter than the average recovery time of the virus. Based on this, all infected individuals remain infected in the population throughout the planning horizon.

Proportion of the number of these new infections to the hospital's share of patients living in the city indicates the increase in the ratio of infectious individuals in the neighborhood of hospital h at the beginning of period t. Following this idea $\alpha_{h,t}$, where $t \geq 2$, is given in Eq. (5).

$$\alpha_{h,t} = (\alpha_{h,t-1})\left(1+\frac{R}{10}\right) + \frac{Z_{h,t-1}W^{t-1}_{h,1}}{Pop_h} \tag{5}$$

Given that the supply for masks is quite scarce during a pandemic, they should be allocated to a set of hospitals considering fairness between these hospitals. To this end, a fairness function which takes the form of a DCF is established using shortage values as a metric. In our case, DCF is caused by the lack of access to proper protective equipment which cause probability of infection to increase for individuals. Deprivation time (waiting time for PPE) and distribution vector (X) (and hence the shortage amounts) are the main inputs to DCF. The rate of increase in deprivation cost gets larger as the deprivation time increases. Therefore, it is expected that a DCF should be monotonic, non-linear and convex with respect to the deprivation time.

By using a proper DCF, aim in this study is to minimize the number of consecutive periods for which demand is poorly satisfied. Each period is evaluated to specify a poor service level. In our case, for all hospitals and all time periods, shortage may always occur due to the high scarcity of masks. Therefore rather than taking a binary approach in which any positive shortage amount indicates poor service, we define the service level as the proportion of demand received by the hospital and declare poor service if the demand for a mask type j is met less than a pre-determined proportion (δ) on a period t. Then it is said that the service level is poor for a hospital h; if it is bigger than or equal to the threshold, it is said that the service level is good enough. Therefore, deprivation time can be defined as waiting time for service level to increase to δ again. Assuming that the beginning deprivation cost values ($DC^0_{h,j}$) are zero, deprivation ($DC^t_{h,j}$) is the accumulated shortage until a good service level as Eq. (6) shows.

$$DC^t_{h,j} = \begin{cases} DC^{t-1}_{h,j} + U^t_{h,j}, & \text{If } U^t_{h,j} \geq \left\lfloor \delta W^t_{h,j} \right\rfloor + 1 \\ 0, & \text{Otherwise} \end{cases} \quad \forall t \in T, \forall h \in H, \forall j \in J \tag{6}$$

A binary variable $SL^t_{h,j}$ is defined based on Eq. (7) indicating the quality of the service level (value 1 means poor service whereas 0 means good service).

$$SL^t_{h,j} = \begin{cases} 1, & \text{If } U^t_{h,j} \geq \left\lfloor \delta W^t_{h,j} \right\rfloor + 1 \\ 0, & \text{Otherwise} \end{cases} \quad \forall t \in T, \forall h \in H, \forall j \in J \tag{7}$$

Then $DC^t_{h,j} = (DC^{t-1}_{h,j} + U^t_{h,j})SL^t_{h,j}$, $\forall h \in H, t \in T$.

An instance for a hospital h and mask type j with $\delta = 20\%$ is shown in Table 4, where $|T| = 7$. Demand of hospital h for mask type j is assumed to be constant and equals to 50 for all periods. Then, if shortage for a period is less than or equal to $20\% \times 50 = 10$, required service level is achieved and deprivation does not occur. If shortage is more than or equal to 11 units, deprivation occurs. One of

Table 4
An instance to calculate deprivation cost.

$W^t_{h,j} = 50\ \forall t,\ \delta = 20\%$							
Periods	1	2	3	4	5	6	7
$X^t_{h,j}$	35	20	25	43	50	32	42
$U^t_{h,j}$	15	30	25	7	0	18	8
$SL^t_{h,j}$	1	1	1	0	0	1	0
$DC^t_{h,j}$	15	15+30	15+30+25	0	0	18	0

the objective functions of the allocation inventory model is determined as minimizing the maximum deprivation cost among the hospitals.

In addition to fairness, disease spread is another performance measure that is affected by the mask allocation decisions. Number of infections due to medical procedures conducted in hospitals should be minimized to decelerate the spreading of the disease. Ratio of infected doctors and infected patients can be used as the objective functions for this purpose. Preliminary work shows that these two objective functions are highly correlated as one can expect. Hence one of these objective functions is used in the mathematical model. As health care workers should be prioritized during pandemics and epidemics (Binkley and Kemp, 2020; Emanuel et al., 2020), ratio of infected doctors accumulated during the planning horizon is selected as an objective function for the mathematical model. To further establish equity, all objective functions are formed using the Rawlsian approach.

Considering the notation introduced earlier, the multi-objective multi–period non-linear allocation inventory problem can be modeled as in Eqs. (8)–(25) given in Box I.

Objective function (8), Obj_Y, minimizes the maximum number of infected health workers among hospitals during the planning horizon as a metric of disease spread due to inadequate PPE use of hospitals whereas objective function (9), Obj_{DC}, is to minimize the maximum deprivation cost over hospitals. Constraints (10) ensure that all daily supply is distributed and Constraints (11) are the inventory balance equations. Constraints (12) ensure that shortage and inventory cannot occur together for a specific hospital and a specific time period and Constraints (13) indicate the beginning inventory levels. Constraints (14) and (15) calculate deprivation cost related to each mask type for each hospital for the periods where service level is poor. Otherwise, they assign deprivation cost as zero. The service level is labeled as poor or good in constraints (16) and (17). Constraints (18) are to find infection rate during an appointment due to an infectious patient while constraints (19) calculate the same rate due to an infected doctor. Constraints (20) indicate the ratio of infected doctors, (21) calculates ratio of infected arriving patients and (22) specifies ratio primary infections during appointments. Constraints (23)–(25) are the domain constraints.

5. Solution approaches

In this section we elaborate on the solution approach that we use to solve the bi-objective mask distribution problem discussed in Section 4. Our aim is to determine a set of good quality solutions with respect to the two objectives, to be presented to the decision makers for further comparison.

Note that due to the trade-off between the two objectives, the problem will not have a single solution that performs best with respect to both objectives, rather a set of *Pareto solutions* that perform to different degrees in the two criteria. A Pareto solution is a (feasible) solution of the problem such that there is no other (feasible) solution that performs at least as good as it in all criteria, while being strictly better with respect to at least one criterion.

Various exact and heuristic approaches for multi-objective optimization problems are used in the literature to determine the set (or a subset of) exact and approximate Pareto solutions, respectively. One common way of generating Pareto solutions is iteratively solving single objective scalarization problems, each time with different parameters so as to generate different Pareto solutions. Weighted sum, ϵ-constraint and Tchebycheff scalarization are widely used examples of these scalarizations.

We utilize ϵ-constraint method to solve the non-linear bi-objective mathematical model. Even for small sized instances it is challenging to obtain all non-dominated solutions for such a model in the exact Pareto front. We therefore utilize two heuristic methods: (i) a set of rule-of-thumb policies, which can be applied easily without any computational effort, (ii) a novel meta-heuristic approach, a genetic algorithm (GA) to establish an approximate Pareto frontier.

In the upcoming sections, we provide the details of the rule-of-thumb policies and the customized genetic algorithm as ways to obtain heuristic solutions for the dimensions where solving the non-linear multi-period mathematical model to optimality will be computationally extremely challenging.

5.1. Solving the mathematical model

Solving our mathematical model even with a single objective is quite challenging as it is a highly non-linear mixed integer programming model. To get the exact Pareto solutions, the ϵ-constraint algorithm necessitates solving a sequence of the following two models:

$$\begin{aligned} \min\quad & Obj_{DC} \\ \text{s.t.}\quad & Obj_{DC} \geq \sum_{t\in T}\sum_{j\in J} DC^t_{h,j} && \forall h \in H \\ & \sum_{t\in T} Y_{h,t} \leq \epsilon_1 && \forall h \in H \\ & (10) - (25) \end{aligned}$$

and

$$\begin{aligned} \min\quad & Obj_{Y} \\ \text{s.t.}\quad & Obj_{Y} \geq \sum_{t\in T} Y_{h,t} && \forall h \in H \\ & \sum_{t\in T}\sum_{j\in J} DC^t_{h,j} \leq \epsilon_2 && \forall h \in H \\ & (10) - (25) \end{aligned}$$

These models not only have non-convex quadratic constraints as (12), (15), (17), (18) and (19) but also constraints involving high exponent variables such as (20)–(22). Starting with version 9.0, Gurobi Optimization has been offering a novel bilinear solver feature that is capable of handling non-convex quadratic optimization models to global optimality. Gurobi can also handle powers of variables by piecewise-linear approximation with user controlled piece number information — the higher the number of pieces, the better the approximation. In our preliminary experimentation, this option turned out to be computationally ineffective. Thus, we opted to do handle the variables with high integer exponent values by writing them as a sequence of quadratic products at the expense of increasing the number of variables and constraints. In particular, if our power of variable to handle is x^p where $p = 2^k$ for some positive integer k for simplicity, we add k new variables $y_1, \ldots, y_k$ and the following quadratic equations

$$y_1 = x^2 \text{and } y_i = y^2_{i-1} \text{for } i = 2, \ldots, k$$

to our model. In this fashion y_k will be equal to x^p and any integer exponent p can be handled with $O(log_2\ p)$ additional variables and quadratic constraints.

5.2. Rule-of-thumb policies

We propose some rule-of-thumb policies as basic approaches having the potential to establish a reasonably fair allocation. Such policies may be the preferred by decision makers in real-life applications, owing to their simplicity, ease of implementation and communication. For each such policy, we determine the solution and include this solution to the initial pool of the genetic algorithm as will be explained in Section 5.3.1. Following this, we observe the improvement genetic algorithm makes on these solutions by comparing them to the Pareto optimal solutions the model yields.

$$\min \quad \text{Obj}_Y = \max_{h\in H} \sum_{t\in T} Y_{h,t} \tag{8}$$

$$\min \quad \text{Obj}_{DC} = \max_{h\in H} \sum_{t\in T} \sum_{j\in J} DC^t_{h,j} \tag{9}$$

subject to:

$$\sum_{h\in H} X^t_{h,j} = S^t_j \qquad \forall t\in T, \forall j\in J \tag{10}$$

$$I^t_{h,j} - U^t_{h,j} = X^t_{h,j} + I^{t-1}_{h,j} - W^t_{h,j} \qquad \forall t\in T, \forall h\in H, \forall j\in J \tag{11}$$

$$I^t_{h,j} U^t_{h,j} = 0 \qquad \forall t\in T, \forall h\in H, \forall j\in J \tag{12}$$

$$I^0_{h,j} = 0 \qquad \forall h\in H, \forall j\in J \tag{13}$$

$$DC^0_{h,j} = 0 \qquad \forall h\in H, \forall j\in J \tag{14}$$

$$DC^t_{h,j} = (DC^{t-1}_{h,j} + U^t_{h,j}) SL^t_{h,j} \qquad \forall t\in T, \forall h\in H, \forall j\in J \tag{15}$$

$$U^t_{h,j} \geq \left(\left\lfloor \delta W^t_{h,j} \right\rfloor + 1\right) SL^t_{h,j} \qquad \forall t\in T, \forall h\in H, \forall j\in J \tag{16}$$

$$U^t_{h,j}(1 - SL^t_{h,j}) \leq \left\lfloor \delta W^t_{h,j} \right\rfloor (1 - SL^t_{h,j}) \qquad \forall t\in T, \forall h\in H, \forall j\in J \tag{17}$$

$$P^1_{h,t} = \left(1 - \frac{U^t_{h,1}}{W^t_{h,1}}\right)\left(1 - \frac{U^t_{h,2}}{W^t_{h,2}}\right)\beta_1\theta_2 + \frac{U^t_{h,1}}{W^t_{h,1}}\frac{U^t_{h,2}}{W^t_{h,2}}\beta\theta + \left(1 - \frac{U^t_{h,1}}{W^t_{h,1}}\right)\frac{U^t_{h,2}}{W^t_{h,2}}\beta_1\theta + \frac{U^t_{h,1}}{W^t_{h,1}}\left(1 - \frac{U^t_{h,2}}{W^t_{h,2}}\right)\beta\theta_2 \qquad \forall t\in T, \forall h\in H \tag{18}$$

$$P^2_{h,t} = \left(1 - \frac{U^t_{h,1}}{W^t_{h,1}}\right)\left(1 - \frac{U^t_{h,2}}{W^t_{h,2}}\right)\theta_1\beta_2 + \frac{U^t_{h,1}}{W^t_{h,1}}\frac{U^t_{h,2}}{W^t_{h,2}}\theta\beta + \left(1 - \frac{U^t_{h,1}}{W^t_{h,1}}\right)\frac{U^t_{h,2}}{W^t_{h,2}}\theta_1\beta + \frac{U^t_{h,1}}{W^t_{h,1}}\left(1 - \frac{U^t_{h,2}}{W^t_{h,2}}\right)\theta\beta_2 \qquad \forall t\in T, \forall h\in H \tag{19}$$

$$Y_{h,t} = 1 - (1 - P^1_{h,t}\alpha_{h,t})^{\left\lceil \frac{W^t_{h,1}}{W^t_{h,2}} \right\rceil} \qquad \forall t\in T, \forall h\in H \tag{20}$$

$$\alpha_{h,t} = (\alpha_{h,t-1})\left(1 + \frac{R}{10}\right) + \frac{Z_{h,t-1} W^{t-1}_{h,1}}{Pop_h} \qquad \forall t\in T\setminus\{1\}, \forall h\in H \tag{21}$$

$$Z_{h,t} = (1 - \alpha_{h,t})(Y_{h,t} P^2_{h,t}) \qquad \forall t\in T, \forall h\in H \tag{22}$$

$$X^t_{h,j}, U^t_{h,j}, I^t_{h,j}, DC^t_{h,j}, Y_{h,t}, Z_{h,t}, \alpha_{h,t}, P^1_{h,t}, P^2_{h,t} \geq 0 \qquad \forall t\in T, \forall h\in H, \forall j\in J \tag{23}$$

$$X^t_{h,j}, U^t_{h,j}, I^t_{h,j}, DC^t_{h,j} \text{ integer} \qquad \forall t\in T, \forall h\in H, \forall j\in J \tag{24}$$

$$SL^t_{h,j} \in \{0,1\} \qquad \forall t\in T, \forall h\in H, \forall j\in J \tag{25}$$

Box I.

A naive approach namely, *Equal Split* policy, would be equally splitting the supply to the hospitals for each time period. *Proportional Split* policy is distributing masks to each hospital in proportion to the population that they give service to (Pop_h). A last-in-first-receives distribution strategy is analyzed as a third policy, namely $LIFR_\delta$, meaning that if a hospital is visited last in the current period, it will be visited first in the next period. Such a strategy resembles cyclic priority queues with dynamically changing priorities of channels i.e. hospitals in our case (Browne and Yechiali, 1989). The priorities for the first period are determined based on the demand levels. Based on this ordering, for each hospital, 80% of the demand ($\left\lceil (1-\delta) * W^t_{h,j} \right\rceil$) is satisfied when the supply is sufficient to avoid deprivation. If the supply is not enough the hospital is given what is available. In the next period, the visiting order is reversed. A similar policy can be applied by distributing all of the supply to the first visited hospital in each period, which will be referred as $LIFR_{all}$.

Let $O^t_{h,j}$ be the visiting order of hospital h in period t for mask type j where $O^t_{h,j} \in \{1,\ldots,|H|\}$. Ordering for the first period is initialized in such a way that hospitals with higher demands are visited earlier. Based on the last-in-first-receives strategy, Eq. (26) calculates the orders for the other periods.

$$O^t_{h,j} = |H| - O^{t-1}_{h,j} + 1 \tag{26}$$

Let $\bar{H}^t_{h,j}$ be the set of hospitals that are visited before hospital h in period t for mask type j as given in (27).

$$\bar{H}^t_{h,j} = \{h' \in H | O^t_{h',j} \leq O^t_{h,j} - 1\} \tag{27}$$

Distribution amounts with respect to each rule-of-thumb policy are given in Table 5. Allocation vectors for the *Equal Split* and *Proportional Split* policies take integer values by rounding down operations and distributing an arbitrary hospital ($|H|th$ hospital) the amount left from the other hospitals. For instance with 100 units of supply and 3 hospitals, *Equal Split* policy yields the distribution vector $(33, 33, 34)$.

Table 5
Distribution amounts with respect to rule-of-thumb policies.

Policies	Distribution amounts
Equal Split	$X^t_{h,j} = \lfloor \frac{S^t_j}{\lvert H\rvert} \rfloor \ \forall h\in H\setminus\{\lvert H\rvert\},\ X^t_{\lvert H\rvert,j} = S^t_j - \sum_{h=1}^{\lvert H\rvert-1} X^t_{h,j}$
Proportional Split	$X^t_{h,j} = \lfloor \frac{S^t_j Pop_h}{\sum_{h\in H} Pop_h} \rfloor \ \forall h\in H\setminus\{\lvert H\rvert\},\ X^t_{\lvert H\rvert,j} = S^t_j - \sum_{h=1}^{\lvert H\rvert-1} X^t_{h,j}$
$LIFR_\delta$	$X^t_{h,j} = \max\{0, \min\{S^t_j - \sum_{h'\in \bar{H}^t_{h,j}} X^t_{h',j}, \left\lceil (1-\delta) W^t_{h,j} \right\rceil\}\}$
$LIFR_{all}$	$X^t_{h,j} = \begin{cases} S^t_j, \text{ if } \bar{H}^t_{h,j} = \emptyset \\ 0, \text{ else} \end{cases}$

5.3. The proposed genetic algorithm

Inspired by the evolutionary processes seen in the nature, the genetic algorithms (GA) fall into the class of hyper-heuristics. Since

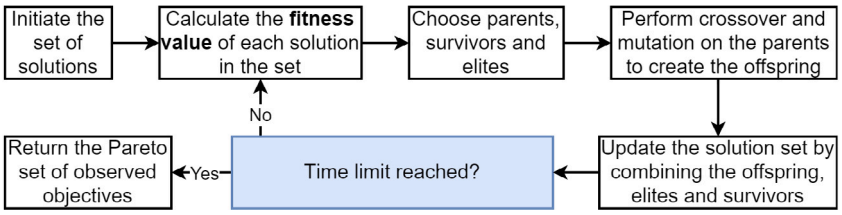

Fig. 1. Flow chart of the genetic algorithm proposed.

they can be applied to any problem as long as a proper solution representation can be found on which the algorithm operators can work, there have been various applications of regarding these algorithms (Mitchell, 1996; Deb et al., 2002). In multi-objective problems, a transformation of the objectives into a single one is required in order for conventional (single objective) GA operators to work. The scalarization can be achieved simply by applying a weighted sum to the objectives or their normalized values (Murata et al., 1996; Qu and Suganthan, 2010). Genetic algorithms are used to obtain good quality heuristic solutions (also referred to as approximate) solutions to problems that are difficult to solve due to various reasons such as being prohibitively large-sized or involving non-linearity. When applied to multi-objective programming problems, the algorithm returns a set of approximate Pareto solutions, i.e. solutions that may not lie on the true (exact) Pareto frontier. The general procedure followed by the proposed genetic algorithm is given in Fig. 1. We provide details of each step in the following sections.

5.3.1. Solution representation and initial population

A matrix K of size $|T|\times|H|\times|J|$ with values $[K^t_{h,j}]$ between [0, 1] is chosen as the solution representation. The algorithm starts with an initial population, which is the set of randomly generated feasible solutions and solutions obtained by the pre-determined distribution policies including the aforementioned rule-of-thumb strategies. Additionally, alternative orderings are possible. One of such alternatives, which will be referred as $Rolling_\delta$, adopts the allocation amounts given by the policy $LIFR_\delta$ with a different ordering scheme. Consider a problem with $|H|$ hospitals having $|H|!$ options for the ordering of the first period. As Equivalence (28) indicates, $Rolling_\delta$ increases orders by c units after each period $t-1$ where $c\in\{1,\dots,|H|-1\}$ leading $|H|-1$ options for this increment, given that $t\geq 2$.

$$O^{t-1}_{h,j}+c\equiv O^t_{h,j}\ (\text{mod}\ |H|) \tag{28}$$

Number of enumerations is $(|H|!(|H|-1))^2$ for the planning horizon for a set of $|H|$ hospitals and 2 mask types. Due to the computational effort it requires, such an approach is not considered as one of the rule-of-thumb policies. However, this policy is utilized in addition to the rule-of-thumb policies while generating the initial population for the genetic algorithm.

After solutions to the rule-of-thumb policies and the possible $Rolling_\delta$ orderings are calculated, the remaining slots are filled by solutions constructed as follows: $X^t_{h,j}=\bigcup_{j\in J,t\in T}\{\hat{X}^t_{h,j}\}\ \forall h\in H$ where $\hat{X}$ is a randomly picked solution from the existing solutions, for each $j\in J, t\in T$. Number of solutions obtained by $Rolling_\delta$ orderings is limited to ensure the initial population includes at least a pre-determined number of randomly generated solutions.

The mask distributions are scaled so that they sum to 1 for each day and mask type, to enable performing mutation and crossover between the solutions. Future populations are generated recursively; each new population is generated using the selected parents and the survivors of the previous population.

The mask distribution for each hospital, period and mask type is calculated by rounding the multiplication of available number of masks per period and the scaled scores as shown below.

$K^t_{h,j}$: score of hospital h at period t for mask type j in the solution.

$\forall t\in T, h\in H, j\in J$

$$I^0_{h,j}\leftarrow 0 \qquad \forall h\in H,\forall j\in J \tag{29}$$

$$X^t_{h,j}\leftarrow\left\lfloor\frac{K^t_{h,j}}{\sum_{i\in H}K^t_{i,j}}\times S^t_j\right\rfloor \qquad \forall t\in T,\forall h\in H\setminus\{1\},\forall j\in J \tag{30}$$

$$X^t_{1,j}\leftarrow X^t_{1,j}+S^t_j-\sum_{h\in H\setminus\{1\}}X^t_{h,j} \qquad \forall t\in T,\forall j\in J \tag{31}$$

$$I^t_{h,j}\leftarrow\max\left\{(X^t_{h,j}+I^{t-1}_{h,j}-W^t_{h,j}),0\right\} \qquad \forall t\in T,\forall h\in H,\forall j\in J \tag{32}$$

$$U^t_{h,j}\leftarrow\max\left\{(W^t_{h,j}-X^t_{h,j}-I^{t-1}_{h,j}),0\right\} \qquad \forall t\in T,\forall h\in H,\forall j\in J \tag{33}$$

Eq. (29) initializes the inventories to zero. Eq. (30) calculates the distributed mask amounts to all hospitals except the first one considering inventories of the previous period. Eq. (31) distributes the remaining masks, which might exist due to the floor function, to the first hospital. Eq. (32) calculates the inventories at each period. The solution representation always results in a feasible distribution of masks since it scales the given scores and does not distribute more than the number of available masks per period and mask type. Once the mask distributions are obtained, the remaining variables in the model are calculated, along with the objective values. The input of the fitness function is the two objective function values (8) and (9).

In the following sections, detailed explanations of the steps of the algorithm are provided.

5.3.2. Fitness value calculation

Once the corresponding mask distribution for a solution is found, its fitness value is calculated using one of the objectives depending on how much time has passed since the start of the algorithm: During the first half of the algorithm, Obj_Y (8) is selected as the objective, whereas Obj_{DC} (9) is picked in the remaining half.

5.3.3. Constructing the next population

Once the fitness values are obtained, the next population is constructed depending on these fitness values; the higher the value is, the better the chances of being selected as a survivor or a parent. The next population mainly consists of three types of individuals; survivors (Ting et al., 2009), elites (Ahn and Ramakrishna, 2003) and offspring (Jebari et al., 2013) (see Fig. 2). Survivors and elites are the solutions that are transferred directly from the previous population, they differ in terms of the selection process.

The selection operator represents the 'survival of the fittest' rule seen in the evolutionary process, where the solutions with better fitness values have higher chances of having their characteristics transferred to the next generation. The corresponding selection algorithms are used for determining the parent pairs (Jebari et al., 2013) and survivors (Ting et al., 2009) of the next population.

5.3.4. Parent pairs and offspring

From the evolutionary perspective, the parents are utilized to represent the reproduction procedure. In GA, each parent pair undergoes a crossover operation, which recombines the solutions and results in a pair of two different solutions, called offspring. Then the mutation operator is applied to the offspring, individually. Objective values of

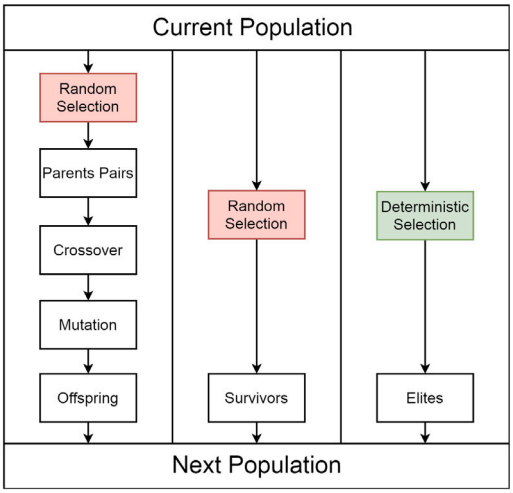

Fig. 2. Generation procedure for the next population.

each offspring has to be calculated again, as they are generated in a random manner.

Each pair is generated by randomly selecting one solution at a time, without replacement, so that no solution is paired with itself. A solution may be selected as a parent in many pairs. The selection probability is determined by the fitness value, which is calculated as described in Section 5.3.2.

Offspring are the individuals that are created by randomly performing crossover on the selected parent pairs. Crossover can be applied with a probability as well, meaning that not every offspring will be a product of a crossover operation, instead they will be same as their parent before the mutation operator.

Mutation operator is then applied to each of the resulting offspring, where a Gaussian noise with mean of 0 and variance σ_{mut} is applied to each index as follows:

^{c}O : Offspring obtained from the crossover operation

K : New individual ready to be added into the next population

$$K^{t}_{h,j} = \min\{1, \max\{0, {}^{c}O^{t}_{h,j} + \mathcal{N}(0, \sigma_{\text{mut}})\}\} \quad \forall t \in T, h \in H, j \in J \qquad (34)$$

which ensures that each index stays within range of [0, 1]. The mutation operator has two important roles:

- **Exploration of the search space**. The crossover operator results in solutions that are convex and/or dimensional combinations of the existing solutions hence allows limited exploration of the solution space. Mutation increases exploration of the search space by making small random changes on the solutions.
- **Maintaining diversity**. The crossover operator reduces the average distance between the individuals of the population, which will eventually result in convergence of the population into one solution. By making small random changes on the solutions, mutation maintains diversity as it changes the population's position in the search space and hence prevents premature convergence.

5.3.5. Survivors and elites

Elites are picked from the best solutions of the population, with a deterministic selection process, i.e. if the elite count is given as 5, the best five solutions of the current population are transferred to the next population without alteration. Elites enable the algorithm to focus more on the parts of the solution space with better objective values.

Similar to the elites, survivors are the solutions that are transferred to the next population without undergoing any alteration process. Unlike elites, survivors are selected using stochastic selectors from the population excluding elites so as to avoid selecting an individual multiple times. They enable the algorithm to preserve some of the good solutions.

From the computational perspective, survivors and elites enable the algorithm to process a higher number of populations, as selected solutions are not altered, their objective values are not calculated again.

5.3.6. Next population & terminating condition & the output

The next population is built by combining the offspring, the elites and the survivors. The objective values are obtained and the terminating condition is checked. If the terminating condition is not met, the algorithm continues its iterations from the fitness value calculation step (5.3.2). Otherwise, it returns the Pareto set of solutions that were observed throughout, which represents an approximation for the true Pareto frontier.

6. Computational analysis

6.1. Data generation

In order to simulate various scenarios and analyze the optimal and the heuristic solutions corresponding to these problem instances, parameters of the mathematical model are generated as shown in Table 6. For all parameters, discrete level sets are used as high, medium and low. In each instance, each parameter is generated using one of these options. The instance with worst case indicates high level for parameters $\beta, \beta_j, \theta, \theta_j, \alpha_{h,1}, \lambda_h$ and low level for parameters $dpat_h, dpop_h, ds^t_j$. Similarly, the instance with best circumstances is the one where parameters $\beta, \beta_j, \theta, \theta_j, \alpha_{h,1}, \lambda_h$ are in the low level and parameters $dpat_h, dpop_h, ds^t_j$ are in high level.

Recall that we consider the allocation problem arising at the beginning of the pandemic where mask scarcity is experienced the most, hence we generated the problem instances accordingly. Inward and outward infection rates of the masks are used as specified by (Eikenberry et al., 2020). Reproduction number is taken from (Wu et al., 2020), which estimates the reproduction number with 95% confidence interval in China in January, 2020. $\alpha_{h,1}$ is calculated using the number of positive cases in Turkey during the pandemic phase and the population of the country.

In order to generate $W^t_{h,j}$ (daily number of arriving outpatients) values, additional parameters λ_h (mean of the Poisson distribution for the arriving outpatients) and $dpat_h$ (ratio of doctors to the total number of arriving outpatients for a specific hospital) are used. Similarly, for the parameters Pop_h (number of residents in the neighborhood of each hospital), $dpop_h$ (ratio of number of doctors to the number of individuals that live in the district for each hospital) is used and the ratios ds^t_j (ratio of total daily supply to total daily demand for each mask type) is utilized to generate S^t_j values. The reason for using such additional parameters is to take the relation between some parameters into account. For example, number of outpatients and number of doctors for each hospital should be proportional to the population whereas amount of daily supply should be based on the total daily demand. Therefore, instead of generating these parameters independently from each other, additional parameters are used and generation process is conducted as explained in Algorithm 1.

6.2. Application details for the proposed GA

The genetic algorithms are composed of various different parts with a number of parameters, and there is not an optimal set of parameters that is guaranteed to provide the best performance in every problem. Therefore, in order to fine-tune the genetic algorithm parameters, we utilized another genetic algorithm, whose properties and procedures are described in Appendix B.

Table 6
Parameters.

Parameter		High	Medium	Low
R	Reproduction rate	2.86	2.68	2.47
β	Outward infection rate w/o mask	1	0.995	0.990
β_1	Outward infection rate with mask type 1 (surg. mask)	0.5	0.3	0.1
β_2	Outward infection rate with mask type 2 (resp. mask)	0.3	0.15	0.0
θ	Inward infection rate w/o mask	1	0.995	0.990
θ_1	Inward infection rate of mask type 1 (surg. mask)	0.3	0.2	0.1
θ_2	Inward infection rate of mask type 2 (resp. mask)	0.05	0.025	0.0
$\alpha_{h,1}$	Ratio of infected arriving patients to hospital h at the beginning	0.009	0.006	0.003
λ_h	Incoming patient distribution parameter of hospital h	1000	750	500
$dpat_h$	Doctor to average incoming patient ratio for hospital h	0.1	0.06	0.02
$dpop_h$	Doctor to population ratio for hospital h	0.002	0.0013	0.0006
ds_j^t	Supply to demand ratio for mask type j and period t	0.8	0.6	0.4

6.3. Results

In this section, using the data generation procedures explained in Section 6.1, results for various scenarios are discussed. These scenarios are selected in a way that represents different situations encountered during the pandemic phase. A pessimistic scenario represents a case where the reproduction rate and beginning infected individual ratios around the hospitals, mask infection rates and number of daily visitors to the hospitals are high. Doctor to patient and doctor to population ratios are low, and supply for PPE is scarce in such a scenario. On the other hand, these parameters take reversed values in an optimistic scenario. All parameters take medium values for a neutral scenario. We first observe the Pareto frontiers obtained in each of the optimistic, neutral and pessimistic scenarios with the set of 3 hospitals and 7 days as the length of the planning horizon. The threshold for deprivation cost remains the same (20%) for all of the scenarios. Approximated Pareto fronts are compared with the true Pareto fronts for all scenarios. Finally, resulting distribution schemes of selected optimal solutions, GA solutions and rule-of-thumb policies are discussed in depth for the pessimistic scenario, which is the most likely and challenging one due to insufficient supply and higher infection rates.

Fig. 3 shows the true Pareto and the approximate Pareto respectively obtained by the mathematical model and GA for the three scenarios along with the points returned by rule-of-thumb policies. Table 7 includes the objective function values corresponding to the solutions with best values of the two objective functions, the respective GA solutions and the rule-of-thumb policies. Let us name the objective function vectors corresponding to end points of the exact Pareto as $Best^{DC}$ and $Best^{Y}$ respectively. Note that each such point is a vector of size two, the first element showing the maximum ratio of infected doctors (Obj_Y value) while the second element showing the maximum the deprivation cost across all hospitals (Obj_{DC} value) in that solution. That is, e.g., $Best^{DC} \in \mathbb{R}^2 := (Best_1^{DC}, Best_2^{DC})$ and $Best^{Y} \in \mathbb{R}^2 := (Best_1^{Y}, Best_2^{Y})$. The corresponding points on the approximate Pareto are referred as $GBest^{DC}$ and $GBest^{Y}$. It can be observed from this table that $LIFR_{all}$ does not yield desirable results. For this reason, points obtained by this policy are not shown in Fig. 3.

The mathematical model was allowed to run for 12 h while the GA was allowed 1 h for each scenario. The time limitation of the model was applied as follows: First the range of objective 1 is found ($Best_1^{Y}$, $Best_1^{DC}$), then the epsilon-constraint algorithm (Haimes et al., 1971) is applied with epsilon values incremented by $\frac{Best_1^{DC} - Best_1^{Y}}{10}$ with a time limit of 1.2 h, to ensure that each sub-model is allowed to run for a reasonable time and the Pareto front is uniformly covered. Both the GA and the model were run on a server with 16 GB of RAM (model used HDD to store the node files to avoid RAM limitation, which had a capacity of 400 GB), with Intel(R) Xeon(R) Silver 4210 CPU @ 2.20 GHz. Model was coded in Python 3.8.7 using Gurobi 9.1.0.

We use hypervolume to evaluate the performance of GA in reference to the exact Pareto obtained using the model. Hypervolume, also known as S metric or Lebesgue measure (Zitzler, 1999), is one of the commonly used metrics to assess quality of a Pareto front in the literature (While et al., 2006). Given a reference point r located outside the nadir point, for a solution set N the hypervolume ($H(N)$) is the area of the region: $\cup_{n \in N}\{y \in \mathbb{R}^2 : n \leq y \leq r\}$, as shown in Fig. 4 for the pessimistic scenario.

Table 7
Objective function values obtained by the rule-of-thumb policies and the best points with respect to the two objectives in exact and approximate pareto fronts.

Point	Optimistic scenario	Neutral scenario	Pessimistic scenario
$Best^{DC}$	(0.0039,368)	(0.04434,2001)	(0.6172,5670)
$GBest^{DC}$	(0.0050,422)	(0.04131,2519)	(0.6564,6907)
$Best^{Y}$	(0.0012,1762)	(0.02893,3348)	(0.4295,27463)
$GBest^{Y}$	(0.0017,4525)	(0.03018,8549)	(0.4845,26666)
Equal split	(0.0053,3149)	(0.03578,12391)	(0.5606,19441)
Proportional split	(0.0050,2462)	(0.03568,12196)	(0.5602,19329)
$LIFR_{\delta}$	(0.0050,589)	(0.04811,3368)	(0.7052,19185)
$LIFR_{all}$	(0.0890,23696)	(0.08540,30583)	(1.1491,31805)

The quality of an approximate Pareto set is assessed by the closeness of its hypervolume to the hypervolume of the exact Pareto front. Given that the solution set for GA is N_{GA} and the Pareto optimal solution set is N_{Opt}, the ratio $\frac{H(N_{GA})}{H(N_{Opt})}$ is 0.62, 0.75 and 0.78 respectively for optimistic, neutral and pessimistic scenarios. The hypervolume ratios indicate that Pareto fronts found by GA and model get closer as the scenario worsens and consequently, the customized GA works better under more challenging phases of the pandemic compared to the optimistic cases.

As seen in Fig. 3, in an optimistic scenario, GA yields compatible results to the Pareto optimal solutions in terms of Obj_Y, while returning less compatible values with respect to Obj_{DC}. When the conditions worsen, GA performs better in terms of objective function Obj_{DC}.

As the circumstances get worse the difference between the two extreme solutions of the Pareto set deepens, i.e. the ranges of the two objective function values increase. As a result, solely minimizing the maximum ratio of infected doctors (Obj_Y) leads to very high deprivation cost figures and vice versa. Investigating the whole Pareto frontier provides the decision maker information on the trade-off between the two criteria. For example, it can be seen that a small amount of increase in Obj_Y from its minimum level yields a remarkable decrease in the maximum deprivation cost (Obj_{DC}).

In the optimistic scenario, it is observed that Obj_{DC} value obtained by applying $LIFR_{\delta}$ is significantly close to the best value in that objective. On the other hand, as the scenario gets worse, the performance of $LIFR_{\delta}$ solution with respect to deprivation cost declines.

It is also observed that *Equal Split* and *Proportional Split* yield quite similar results. This is expected as the populations are close for the three hospitals in these instances. These two policies are most appropriate to use when a neutral or pessimistic scenario occurs to obtain acceptable Obj_Y values. However, it should be noted that the resulting Obj_{DC} values are quite high.

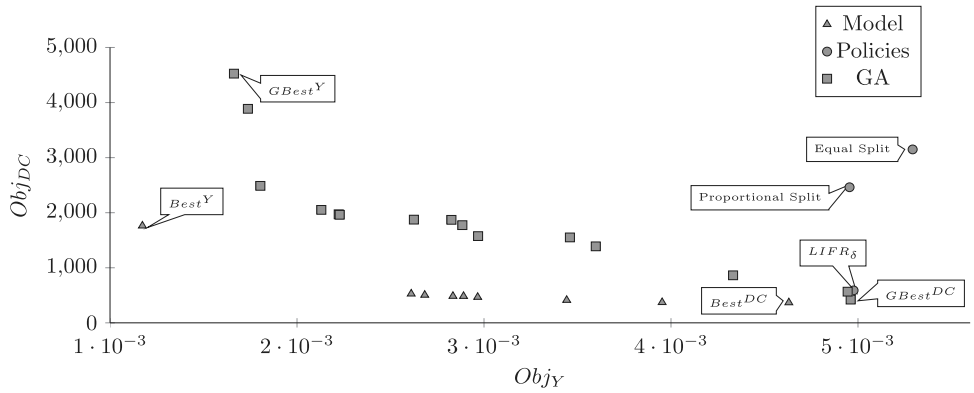

(a) Optimistic Scenario

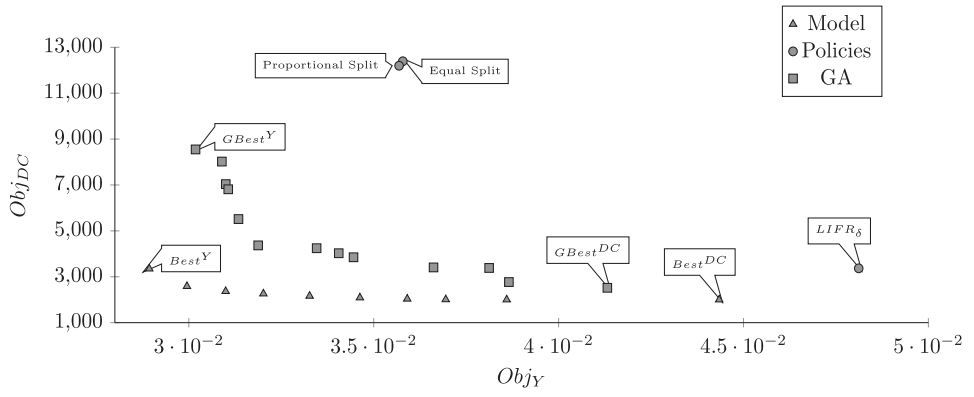

(b) Neutral Scenario

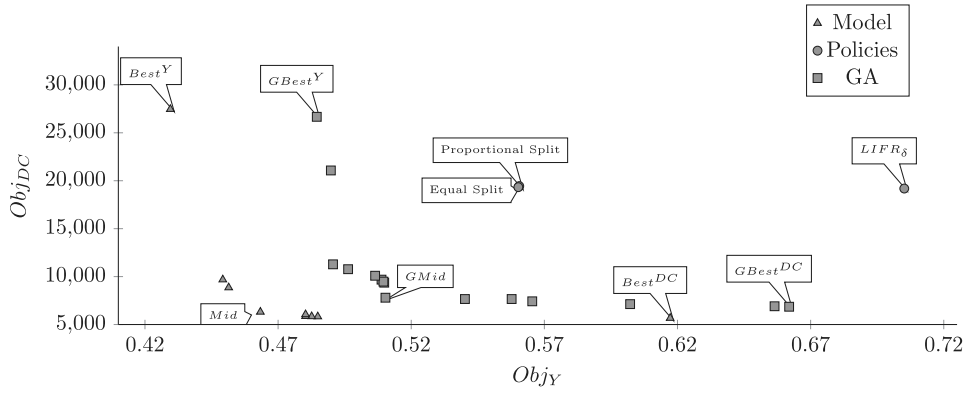

(c) Pessimistic Scenario

Fig. 3. Rule-of-thumb Policies, True Pareto and Approximate Pareto Frontiers obtained by the Mathematical Model and GA. $LIFR_{all}$ results are quite distant from the Pareto frontiers, hence they are not shown.

In order to compare GA with the mathematical model and observe the trade-off between objective functions, sample solutions for a pessimistic instance are analyzed in depth, which consist of two ends ($Best^{DC}, Best^Y, GBest^{DC}, GBest^Y$) and middle points ($Mid, GMid$) of the true and approximate Pareto as shown in Fig. 3c.

Table 8 includes the supply information for mask type 1 (surg. mask) and demand vector for a pessimistic instance with 3 hospitals during 7 periods generated using the values given in Table 6. The supply for mask type 2 (resp. mask) is 169 for all periods and the demand vector for this mask type is $(141, 142, 139)$, respectively, for each hospital and constant throughout the planning horizon since the number of doctors remains the same. Tables C.11–C.13 give the distribution matrix X respectively for the solutions resulted from $Best^{DC} - GBest^{DC}$, $Best^Y - GBest^Y$ and $Mid - GMid$ pairs for the pessimistic scenario.

Table 8
Demand and supply parameters for the pessimistic scenario.

	Periods						
	1	2	3	4	5	6	7
S_1^t	1176	1181	1214	1217	1238	1205	1171
$W_{1,1}^t$	974	962	995	1054	1032	974	1032
$W_{2,1}^t$	993	977	1024	1026	1063	1044	938
$W_{3,1}^t$	971	1012	1016	961	999	993	956

The allocation strategies corresponding to the best solutions with respect to the deprivation cost are quite similar in GA and the mathematical model as seen in Fig. 5. The solutions indicate that starting from a hospital, distributing $(1-\delta)$% of the demand and performing the same

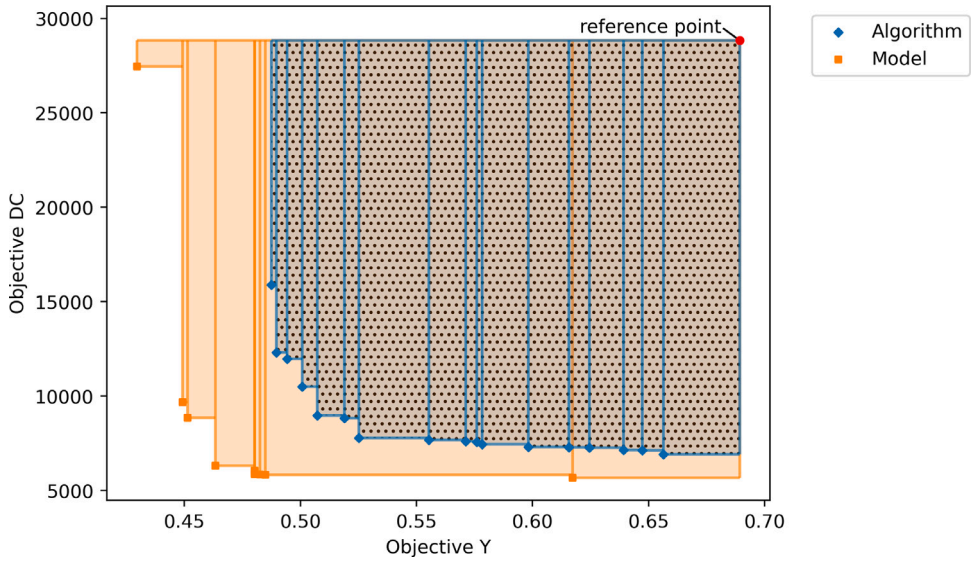

Fig. 4. Areas compared between two different Pareto fronts.

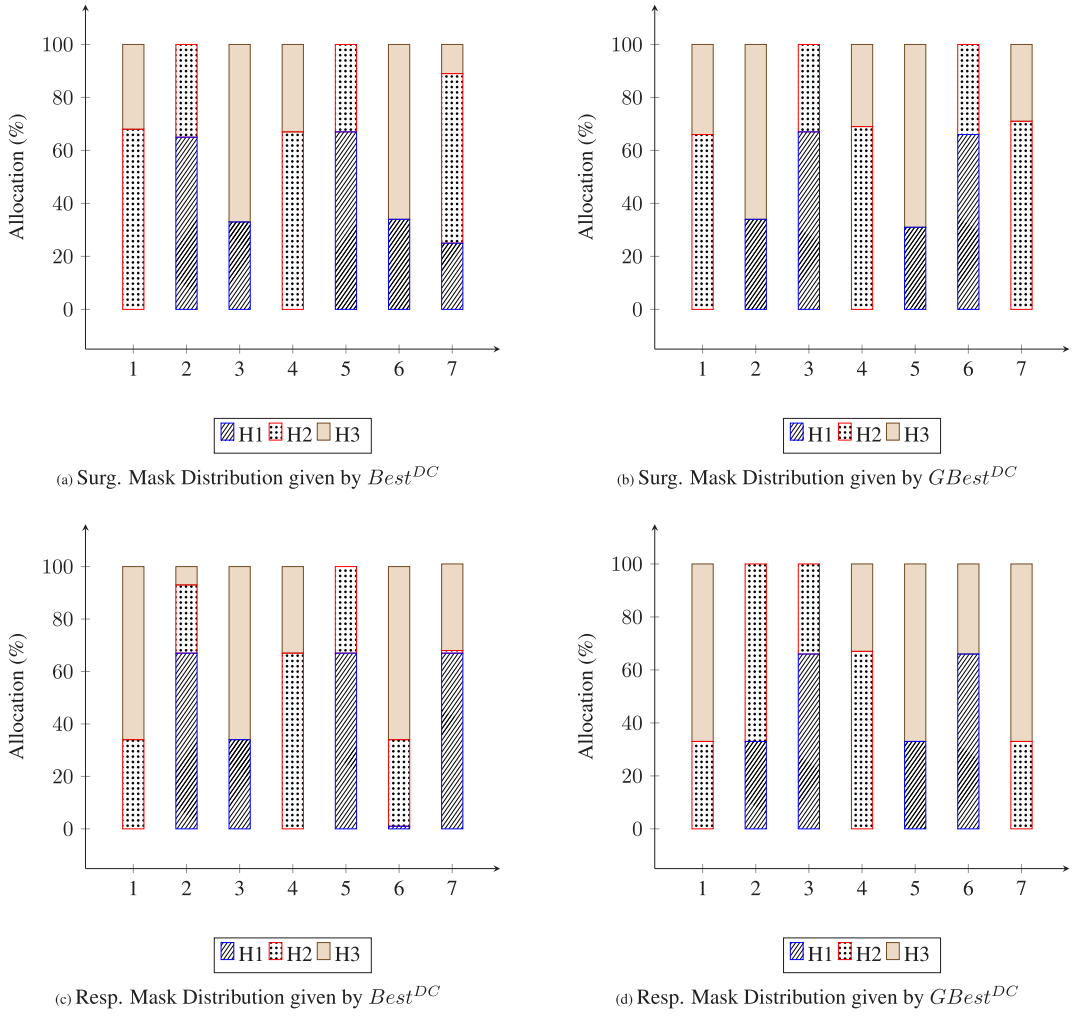

(a) Surg. Mask Distribution given by $Best^{DC}$

(b) Surg. Mask Distribution given by $GBest^{DC}$

(c) Resp. Mask Distribution given by $Best^{DC}$

(d) Resp. Mask Distribution given by $GBest^{DC}$

Fig. 5. Percentage of supply distributed to each hospital for each period obtained by $Best^{DC}$ and $GBest^{DC}$.

activity for a different hospital in each period yields a significant decrease in Obj_{DC} as it prevents consecutive number of periods with high shortage. Therefore, visiting hospitals in a rolling manner throughout the planning horizon and meeting the demand partially based on the service level threshold (δ) is the strategy that should be adopted while minimizing Obj_{DC}. It can be also observed that the amounts distributed

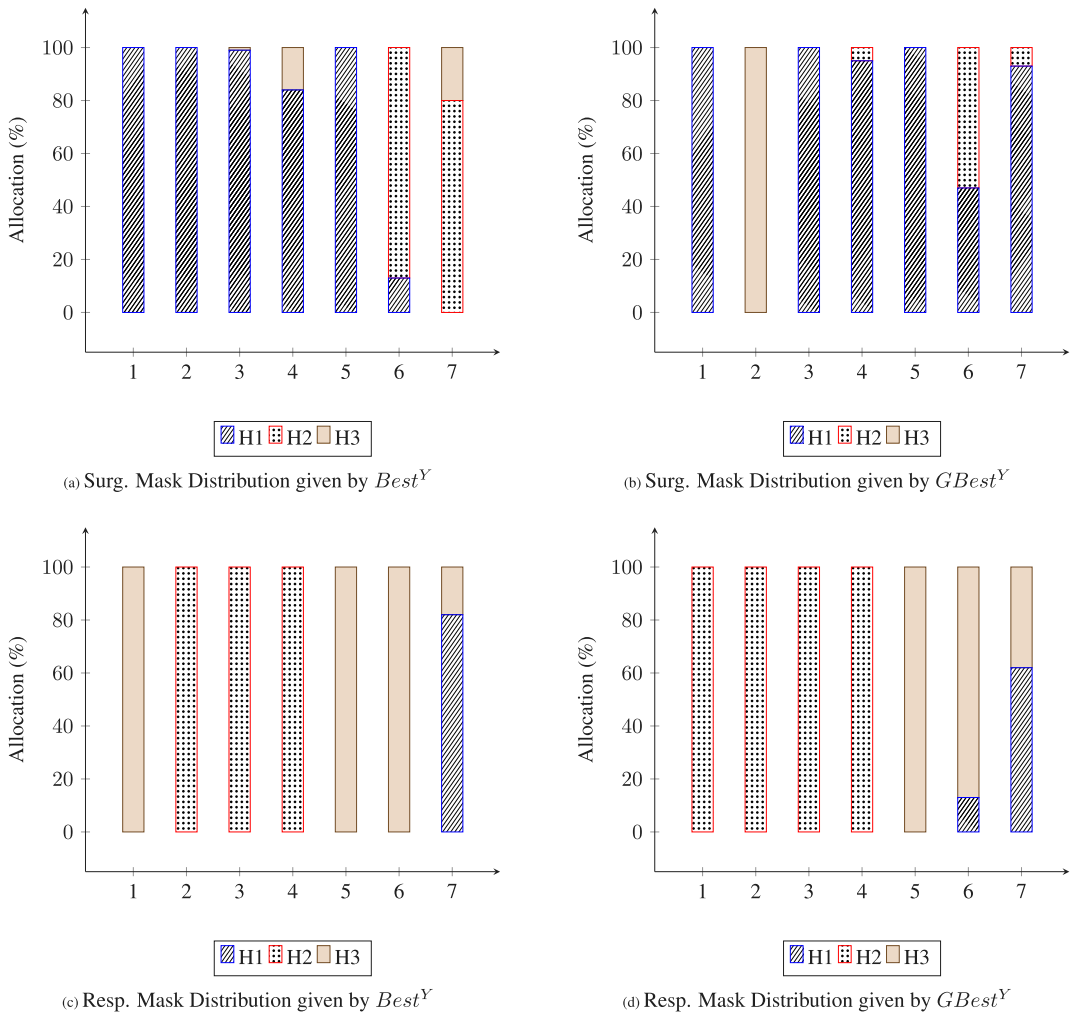

(a) Surg. Mask Distribution given by $Best^Y$

(b) Surg. Mask Distribution given by $GBest^Y$

(c) Resp. Mask Distribution given by $Best^Y$

(d) Resp. Mask Distribution given by $GBest^Y$

Fig. 6. Percentage of supply distributed to each hospital for each period obtained by $Best^Y$ and $GBest^Y$.

are aligned with the ones given by the policy $LIFR_\delta$ with a different a visiting order. There is a regular visiting order followed for surg. mask (each hospital is visited first, second and third in almost same number of time periods).

The percentage of supply allocated to each hospital in each period is shown in Fig. 6 for solutions $Best^Y$ and $GBest^Y$. Note that Obj_Y focuses on equitable protection of the doctors (equity in the outcome) rather than equitable distributing the masks (equity in resource allocation) and it may ensure this through different means. This can be observed in solutions: Almost all of the supply for the surg. mask is allocated to a single hospital (1st hospital in the solutions) whereas the respiratory mask is distributed to another hospital in each period. As a consequence of this strategy, for the doctors in the 1st hospital the infection rate is reduced by equipping the patients with mask rather than the doctors. For the other two hospitals, most of the doctors are provided with masks either at the beginning or at the end of the time horizon. The main difference between two solutions is how the surgical mask is distributed in the second period. While the supply is allocated to 1st hospital in the optimal solution, this amount is given to 2nd hospital in the heuristic solution of GA. Both of the solutions change the strategy in the last periods to make up for the neglected hospitals, i.e., 2nd hospital is given more of surg. mask and 1st hospital is given more of resp. mask in the last periods for both of the solutions. Overall, the distribution schemes are quite similar as Fig. 6 indicates.

The distribution strategy of both the mathematical model and GA while minimizing Obj_Y is aligned with the $LIFR_{all}$ in terms of the distributed amounts. Namely, allocating almost all of the supply to a single hospital for each mask type in each period is common for solutions obtained by the model, GA and $LIFR_{all}$. Although last-in-first-receives ordering is not utilized in the optimal and the heuristic solutions unlike $LIFR_{all}$, the similarity indicates that variants of $LIFR_{all}$ with different ordering schemes can be used to improve the objective function Obj_Y.

The percentage of demand satisfied in each period for each hospital is given as $\left(\frac{I^{t-1}_{h,j}+X^t_{h,j}-I^t_{h,j}}{W^t_{h,j}}\right)$. Fig. 7 shows the relationship between the ratio of infected doctors ($Y_{h,t}$) and demand satisfaction rates for each period in the solution of the point $Best^Y$. The most significant observation that can be driven from Fig. 7 is that even though the Obj_Y value mostly depends on the demand satisfaction rate of the doctors rather than the patients, it is possible to control the infection rate of the doctors by fully equipping the patients. Although the doctors are not provided with resp. mask in the first 4 periods for the 1st hospital, increase rate for the non-cumulative ratio of the infected doctors is slow since the demand satisfaction rate of the patients is 1. As 2nd and 3rd hospitals take turns being allocated resp. mask and are not provided with surg. mask, the periods where they do not receive resp. mask result in quite high values of Obj_Y. For this reason, periodic value of the Obj_Y fluctuates for 2nd and 3rd hospitals whereas it has a relatively smaller (due to high demand satisfaction rate for patients) but continuous increase for the 1st hospital.

The analysis of two ends gives us the ability to explain the reason for the trade-off between two objective functions: Trying to meet the

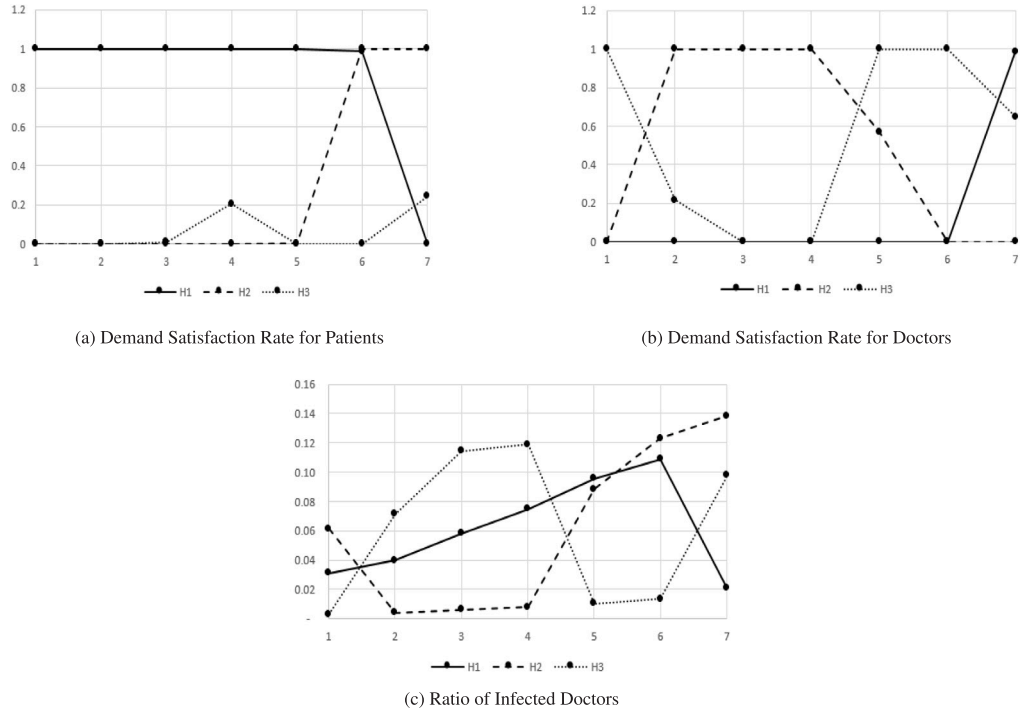

(a) Demand Satisfaction Rate for Patients

(b) Demand Satisfaction Rate for Doctors

(c) Ratio of Infected Doctors

Fig. 7. Demand satisfaction rates and ratio of infected doctors for each period obtained by $Best^Y$.

demand partially based on a pre-determined service level threshold as a way to decrease Obj_{DC}, prevents fully protecting at least one side of the medical appointments namely, patients or doctors. This results in higher Obj_Y values. On the other hand, fully covering at least one of these parties for each hospital would yield a rapid increase in the deprivation cost values for the other hospitals since the demand for at least one mask type is unsatisfied. When a pessimistic scenario occurs, supply to demand ratio gets smaller and this trade-off due to unsatisfied demands becomes more significant.

The solutions regarding Mid and $GMid$ balance the two objective functions unlike the end points. In Fig. 8, it is observed that GA solution allocates all supply to a single hospital in the majority of periods, similar to $LIFR_{all}$. On the other hand, the optimal solution resembles a policy that is a combination of $LIFR_{\delta}$ and $LIFR_{all}$ policies. Overall, the solution Mid has a more complicated distribution scheme, which is not induced by any of the rule-of-thumb policies.

7. Conclusion

Public facilities continuing their services during pandemics should prioritize the safety of their medical staff as well as the public health. Even though the disease continues to spread, reducing the transmission rates within the facility is possible with precautions and measures such as PPE usage and source control. Since healthcare is one of the essential services and occasionally requires close-contact medical procedures, hospitals and health centers should be prioritized while allocating PPE resources. Considering the inadequacy of such a resource during the early phases of a pandemic, allocation between the healthcare facilities should be done in a fair and efficient manner. The aim of this paper is to establish such a PPE allocation while (i) minimizing the disease transmission within the hospitals (ii) distributing the shortage which is likely to occur due to scarcity equitably between the hospitals. To this end, a bi-objective non-linear multi-period allocation model is formulated where non-linearity comes from both the spreading scheme of the disease and way of penalizing shortage with an increasing rate using deprivation cost. The non-linear model is solved to optimality for small sized instances whereas a set of simple policies called rule-of-thumb policies and a customized genetic algorithm are proposed for solving larger problems.

In order to resemble possible real life situations during a pandemic, three scenarios are generated using various levels for problem parameters: pessimistic, neutral and optimistic. Both true and approximate Pareto sets are obtained for these scenarios besides the solutions obtained by rule-of-thumb policies. Optimal and heuristic distribution solutions (end points and a middle point from the Pareto sets) are detailed for the pessimistic scenario. The comparison analysis shows that:

- Hypervolume criterion which evaluates the area of two Pareto fronts, shows that the area implied by customized GA is closer to the area of optimal Pareto front and gives more compatible Obj_{DC} range as the scenario worsens. Additionally, the range between best and worst values of objective functions in Pareto sets gets larger in a pessimistic case.
- Deprivation cost can be improved by meeting demand partially based on deprivation cost threshold for a different hospital in each period while the maximum ratio of infected doctors is decreased by maximizing either patient or doctor demand satisfaction rate for each hospital. The latter requires allocating a single type of mask to a hospital throughout the planning horizon and results in higher values of deprivation cost due to the unsatisfied demand of the other mask type.
- Solutions that balance two objective functions give results such as Mid, and are not implied by any of the rule-of-thumb policies.

To the best of our knowledge, there is no OR study that focuses on protective equipment allocation to a set of hospitals considering the effect of this allocation on infections during medical appointments. Although this study fills this gap, it is not free from some limitations and several directions for future work can be proposed. First, the assumption of daily screen tests for doctors can be relaxed and demand for resp. masks can be considered as a variable for each period depending on the previous demand satisfaction rates. Secondly, it is assumed that an infected person starts infecting other people

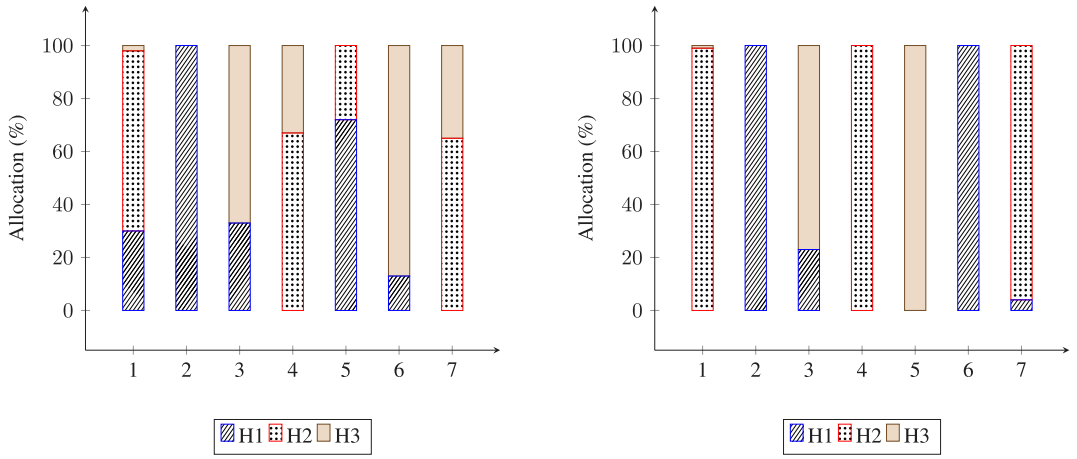

(a) Surg. Mask Distribution given by Mid

(b) Surg. Mask Distribution given by $GMid$

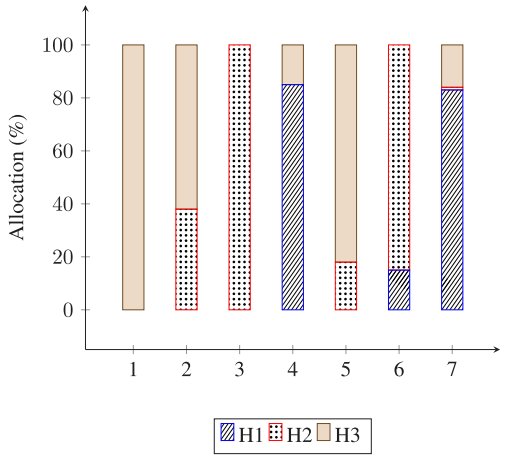

(c) Resp. Mask Distribution given by Mid

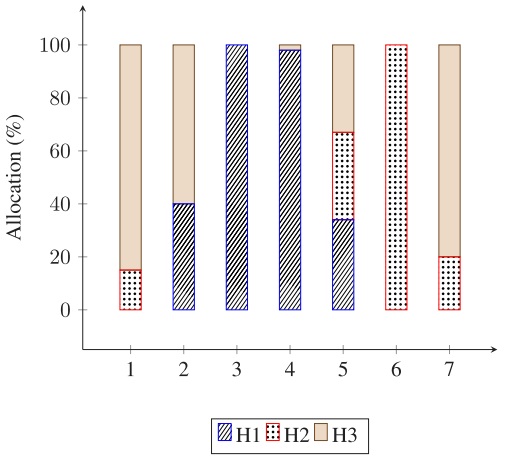

(d) Resp. Mask Distribution given by $GMid$

Fig. 8. Percentage of supply distributed to each hospital for each period obtained by Mid and $GMid$.

immediately. Various values for the time between infection and infectiousness can be considered as a possible direction for future work. Lastly, although the allocation model is constructed as deterministic, a decision maker is likely to encounter uncertainties in such a real-life problem. For instance, infection rates are mostly determined by usage of PPE (e.g. higher when not worn properly). Therefore, methods such as stochastic optimization and robust programming can be used to capture such uncertainties.

CRediT authorship contribution statement

Zehranaz Dönmez: Methodology, Writing – original draft, Formal analysis. **Serkan Turhan:** Methodology, Software, Writing – original draft. **Özlem Karsu:** Writing – review & editing, Validation, Formal analysis. **Bahar Y. Kara:** Conceptualization, Supervision, Writing – review & editing. **Oya Karaşan:** Software, Supervision, Writing – review & editing.

Acknowledgments

Part of the work of the second author was carried out at the Department of Industrial Engineering, Bilkent University.

The authors would like to thank the editors and two anonymous reviewers for their insightful comments and feedback.

Appendix A. Generating hospital parameters

Algorithm 1: Generating the hospital related data

Input: $|T|, |H|, \lambda_h, ds_j^t, dpat_h, dpop_h$
Output: $S_j^t, W_{h,1}^t, W_{h,2}^t, Pop_h$

/* incoming patients */
for $h \in H, t \in T$ **do**
  $W_{h,1}^t = Poisson(\lambda_h)$
/* available doctors */
for $h \in H$ **do**
  $W_{h,2} = \sum_{t \in T} W_{h,1}^t \times dpat_h$
/* populations */
for $h \in H$ **do**
  $Pop_h = \frac{W_{h,2}}{dpop_h}$
/* available number of masks */
for $t \in T$ **do**
  /* surg. mask */
  $S_1^t = ds_1^t \times \sum_{h \in H} W_{h,1}^t$
  /* resp. mask */
  $S_2^t = ds_2^t \times \sum_{h \in H} W_{h,2}$
return $S_j^t, W_{h,1}^t, W_{h,2}^t, Pop_h$

Appendix B. Fine tuning genetic algorithm

We propose a new genetic algorithm in order to fine tune the parameters of the main algorithm. The details of the fine tuning algorithm are as follows:

B.1. Fine tuning algorithm

The main GA procedures are implemented in the same way as described in Section 5.3. We set population size, offspring count, survivor count and elite count to 100, 50, 20 and 30, respectively. We use Roulette Wheel Selection (Lipowski and Lipowska, 2012) and Tournament Selection with tournament size of 5 (Miller and Goldberg, 1995) as parent and survivor selectors, respectively. The algorithm is terminated if there is no update on the best solution over the last 10 populations. A sample size of 5 and 20 benchmark instances were used to assess the performance of settings, instances can be found in Table B.9. Table B.10 shows the algorithm settings obtained after fine tuning the GA.

Table B.9
Benchmark instances used in the fine-tuning algorithm.

Instance name	T	H	ds^t_1	ds^t_2	Instance name	T	H	ds^t_1	ds^t_2
Instance 1	7	3	89.96%	82.14%	Instance 11	10	4	82.35%	72.49%
Instance 2	7	3	84.8%	64.29%	Instance 12	10	4	68.34%	77.54%
Instance 3	7	4	65.38%	74.92%	Instance 13	10	5	68.77%	82.5%
Instance 4	7	4	74.88%	71.5%	Instance 14	10	5	68.59%	70.03%
Instance 5	7	5	75.27%	78.57%	Instance 15	14	3	54.93%	76.79%
Instance 6	7	5	60.22%	64.26%	Instance 16	14	3	65.01%	73.21%
Instance 7	8	3	57.15%	82.68%	Instance 17	14	4	67.54%	73.2%
Instance 8	10	3	58.07%	62.36%	Instance 18	14	4	52.62%	76.91%
Instance 9	10	3	43.94%	80%	Instance 19	14	5	59.99%	85.71%
Instance 10	10	3	68.41%	77.6%	Instance 20	14	5	52.39%	83.92%

Table B.10
Fine-tuned genetic algorithm properties.

Parameter name	Parameter value
Population size	361
Time limit	3600 s
Survivor count	171
Elite count	90
Offspring count	100
Parent selection	Tournament selector with a size of 73
Survivor selection	Truncation selector (Crow and Kimura, 1979)
σ_{mut} (Mutator Variance)	0.63
Crossover operator	Convex combination

B.1.1. Initial population

The initial pool of algorithm settings is generated using the following random distributions and set of candidate parameters:

- **Population Size:** Random integer between 10 and 1000.
- **Offspring, survivor and elite count:** Population size is randomly distributed to each parameter using Algorithm 2 .
- **Mutation parameter** σ_{mut}: U(0, 1).
- **Crossover probability:** Randomly drawn from {0, U(0, 1), 1}. By setting the mating chance as zero, only the mutation operator alters the population, which may produce better results by saving processing time.
- **Crossover operator:** Randomly selected as one of the following: Single Point, Two Point, Uniform with swap probability drawn from U(0,1), and convex combination crossover (Hasançebi and Erbatur, 2000; Hamid et al., 2019).
- **Parent and survivor selectors:** Randomly selected as one of the following:
  - Roulette Wheel Selection (Lipowski and Lipowska, 2012).
  - Tournament Selection (Miller and Goldberg, 1995). Tournament size = $\lfloor population\_size \times ratio \rfloor$, where ratio: U(0, 1).
  - Linear Rank Selection (Shukla et al., 2015). Parameter: U(0, 2).
  - Exponential Rank Selection (Shukla et al., 2015). Smoothing coefficient: U(0, 1).
  - Truncation Selection (Crow and Kimura, 1979).
- **Weight Policy:** The fine-tuning algorithm considers different fitness value calculation techniques in the form of weighted sum functions of the normalized objective function values. The fine tuning algorithm checks the performance of the following weight selection strategies:
  - Pre-determined Weights: $(\omega, 1-\omega)$, where $\omega = \frac{x}{\Delta} \forall x \in \{1, 2, \ldots, \Delta\}$ with Δ randomly selected from {1, 2, ..., 10}. Weights are updated following the same order, with each set having equal amount of run time.
  - Random Weights: $(\omega, 1 - \omega)$ where $\omega \sim U(0, 1)$. Weights are randomized after every N populations. N is randomly selected from {10, 20, 50, 75, 100, 125, 150, 200, 300, 400} for a setting.

We implemented the fine-tuning algorithm for a month and observed that best results are obtained under the pre-determined weights policy with $\Delta = 2$. Hence we use this policy in our main experiments. This policy implies that the algorithm will focus on the first objective in the first half, while switching to the other objective in the second half in fitness value calculations.

B.1.2. Fitness value calculation

Fitness values indicate the quality of the Pareto front found by each setup compared to the other settings in the population. The calculation is shown in Algorithm 3.

B.1.3. Crossover and mutation

After the selection process, algorithm follows the same rules described in Section 5.3. The algorithm settings are explored by crossover and mutation operators as shown in Algorithms 4 and 5. Due to the immense amount of sub-problems needed to be solved to run this algorithm, it was parallel processed in 20 threads, evaluation of the initial population took 20.8 h and the remaining populations took 10.4 h, because only the offspring were evaluated. Each algorithm setting was run for 150 s for each problem and sample to obtain results in a reasonable time.

B.2.

Algorithm 2: Generating uniformly distributed population properties using a fixed population size

Input: population_size
Output: offspring_count, survivor_count, elite_count
/* constrained uniform-random weight set generation, with set summing up to 1 */
1 weights = {0, U(0,1), U(0,1), 1}
2 sorted_weights = sort(weights)
/* generating the uniformly distributed values, summing up to population_size */
3 offspring_count = $\lfloor (\text{sorted\_weights}_1 - \text{sorted\_weights}_0) \times \text{population\_size} \rfloor$
4 survivor_count = $\lfloor (\text{sorted\_weights}_2 - \text{sorted\_weights}_1) \times \text{population\_size} \rfloor$
5 elite_count = population_size - offspring_count - survivor_count
6 **return** offspring_count, survivor_count, elite_count

B.3.

Algorithm 3: Fitness value generator of the fine-tuning algorithm

Input: population, sample_size, benchmark_instances
Output: fitness_values
/* Initialization */
fitness_values = {0 ∀ solution ∈ population}
/* Evaluation */
for benchmark_instance ∈ benchmark_instances **do**
  Pareto_fronts = {∅∀solution ∈ population}
  /* Sample each solution and calculate the Pareto front */
  for solution ∈ population **do**
    for sample ∈ {1, 2, ..., sample_size} **do**
      sampled_Pareto_front = solve_instance_with_settings(solution, benchmark_instance)
      $\text{Pareto\_fronts}_{\text{solution}}$ = sampled_Pareto_front ∪ $\text{Pareto\_fronts}_{\text{solution}}$
    $\text{Pareto\_fronts}_{\text{solution}}$ = efficient_solutions $(\text{Pareto\_fronts}_{\text{solution}})$
  /* Increment the fitness values by the number of efficient points in the Pareto front of solutions obtained by every solution for this benchmark instance */
  population_Pareto_front = efficient_solutions $\left(\bigcup_{\text{solution}\in\text{population}} \text{Pareto\_fronts}_{\text{solution}}\right)$
  for solution ∈ population, efficient_solution ∈ $\text{Pareto\_fronts}_{\text{solution}}$ **do**
    if efficient_solution ∈ population_Pareto_front **then**
      $\text{fitness\_values}_{\text{solution}}$ += 1
return fitness_values

B.4.

See Algorithm 4.

B.5.

See Algorithm 5.

Appendix C. Solutions obtained by end points and middle points of the optimal and approximate pareto fronts for the pessimistic scenario

C.1.

See Table C.11.

C.2.

See Table C.12.

Algorithm 4: Crossover operator used in the fine-tuning algorithm

Input: $\text{Parent}^1, \text{Parent}^2$
Output: $\text{Offspring}^1, \text{Offspring}^2$
/* Initialization */
$\text{Offspring}^1 = \text{Parent}^1$
$\text{Offspring}^2 = \text{Parent}^2$
/* Recombine the population size properties */
for parameter ∈ {offspring_count, survivor_count, elite_count} **do**
  $\phi = U(0, 1)$
  Offspring^1.parameter = $\lfloor \phi \times \text{Parent}^1.\text{parameter} + (1-\phi) \times \text{Parent}^2.\text{parameter} \rceil$
  Offspring^2.parameter = $\lfloor (1-\phi) \times \text{Parent}^1.\text{parameter} + \phi \times \text{Parent}^2.\text{parameter} \rceil$
/* Re-adjust the population size parameters */
Offspring^1.population_size = $\sum_{\text{parameter}\in\{\text{offspring\_count},\ \text{survivor\_count},\ \text{elite\_count}\}} \text{Offspring}^1.\text{parameter}$
Offspring^2.population_size = $\sum_{\text{parameter}\in\{\text{offspring\_count},\ \text{survivor\_count},\ \text{elite\_count}\}} \text{Offspring}^2.\text{parameter}$
/* Recombine the crossover and selection operators */
for operator ∈ {crossover_operator, parent_selection_operator, survivor_selection_operator} **do**
  if Offspring^1.operator = Offspring^2.operator **then**
    /* Recombine the parameters of the operators, if they are the same type */
    $\phi = U(0, 1)$
    Offspring^1.operator.parameter = $\phi \times \text{Parent}^1.\text{operator.parameter} + (1-\phi) \times \text{Parent}^2.\text{operator.parameter}$
    Offspring^2.operator.parameter = $(1-\phi) \times \text{Parent}^1.\text{operator.parameter} + \phi \times \text{Parent}^2.\text{operator.parameter}$
  else
    /* Swap operators with a probability of 25% */
    if $U(0, 1) \le 0.25$ **then**
      Offspring^1.operator = Parent^2.operator
      Offspring^2.operator = Parent^1.operator
/* Weight policy */
if $U(0, 1) \le 0.1$ **then**
  Offspring^1.weight_policy = Parent^2.weight_policy
  Offspring^2.weight_policy = Parent^1.weight_policy
return $\text{Offspring}^1, \text{Offspring}^2$

C.3.

See Table C.13.

Algorithm 5: Mutation operator used in the fine-tuning algorithm

Input: Offspring
Output: Offspring^1
/* Initialize */
Offspring^1 = Offspring
/* Mutate the population size while holding the offspring, survivor and elite ratio the same */
if $U(0,1) \leq 0.10$ **then**
  Offspring^1.population_size = $\lceil U(10, 1000) \rceil$
  for parameter $\in$ {offspring_count, survivor_count} **do**
    Offspring^1.parameter = $\lfloor$Offspring.parameter $\times \frac{\text{Offspring}^1\text{.population\_size}}{\text{Offspring.population\_size}} \rfloor$
  Offspring^1.elite_count = Offspring^1.population_size − Offspring^1.offspring_count − Offspring^1.survivor_count
/* Mutate the offspring, survivor and elite ratios */
if $U(0,1) \leq 0.20$ **then**
  /* Call Algorithm 2 */
  Offspring^1.offspring_count, Offspring^1.survivor_count, Offspring^1.elite_count = Algorithm 2(Offspring^1.population_size)
/* Mutation parameter */
if $U(0,1) \leq 0.10$ **then**
  Offspring^1.mutation_parameter = $U(0,1)$
/* Crossover probability */
if $U(0,1) \leq 0.20$ **then**
  Offspring^1.crossover_probability = $random\_choice(\{0, U(0,1), 1\})$
/* Crossover and selection operators */
for operator $\in$ {crossover_operator, parent_selection_operator, survivor_selection_operator} **do**
  if $U(0,1) \leq 0.05$ **then**
    Offspring^1.operator = GenerateRandomOperator(operator))
/* Weight policy */
if $U(0,1) \leq 0.1$ **then**
  Offspring^1.weight_policy = GenerateRandomPolicy()
return Offspring^1

Table C.11
Distribution amounts X given by the solutions $Best^{DC}$ and $GBest^{DC}$.

	Hospital	Mask type	Periods						
			1	2	3	4	5	6	7
$Best^{DC}$	1	Surg.	0	770	401	0	826	410	296
		Resp.	0	113	57	0	113	2	113
	2	Surg.	795	410	0	821	412	0	751
		Resp.	57	44	0	114	56	55	1
	3	Surg.	381	1	813	396	0	795	124
		Resp.	112	12	112	55	0	112	55
$GBest^{DC}$	1	Surg.	0	399	813	0	386	795	0
		Resp.	0	56	112	0	55	112	0
	2	Surg.	780	0	401	844	1	410	826
		Resp.	55	113	57	113	0	0	55
	3	Surg.	396	782	0	373	851	0	345
		Resp.	114	0	0	56	114	57	114

Table C.12
Distribution amounts X given by the solutions $Best^{Y}$ and $GBest^{Y}$.

	Hospital	Mask type	Periods						
			1	2	3	4	5	6	7
$Best^{Y}$	1	Surg.	1176	1181	1205	1021	1235	161	0
		Resp.	0	0	0	0	0	0	139
	2	Surg.	0	0	0	0	3	1044	938
		Resp.	0	169	169	169	0	0	0
	3	Surg.	0	0	9	196	0	0	233
		Resp.	169	0	0	0	169	169	30
$GBest^{Y}$	1	Surg.	1176	0	1214	1156	1238	572	1091
		Resp.	0	0	0	0	0	22	104
	2	Surg.	0	0	0	61	0	633	80
		Resp.	169	169	169	169	0	0	0
	3	Surg.	0	1181	0	0	0	0	0
		Resp.	0	0	0	0	169	147	65

Table C.13
Distribution amounts X given by the solutions Mid and $GMid$.

	Hospital	Mask type	Periods						
			1	2	3	4	5	6	7
Mid	1	Surg.	358	1181	401	0	894	162	0
		Resp.	0	0	0	144	0	26	141
	2	Surg.	795	0	0	821	344	0	757
		Resp.	0	64	169	0	30	143	1
	3	Surg.	23	0	813	396	0	1043	414
		Resp.	169	105	0	25	139	0	27
$GMid$	1	Surg.	0	1181	278	0	0	1205	52
		Resp.	0	68	169	165	57	0	0
	2	Surg.	1164	0	0	1217	0	0	1119
		Resp.	26	0	0	0	56	169	34
	3	Surg.	12	0	936	0	1238	0	0
		Resp.	143	101	0	4	56	0	135

References

Adida, E., DeLaurentis, P., Lawley, M., 2011. Hospital stockpiling for disaster planning. IIE Trans. 43, 348–362. http://dx.doi.org/10.1080/0740817X.2010.540639.

Ahn, C., Ramakrishna, R., 2003. Elitism-based compact genetic algorithms. IEEE Trans. Evol. Comput. 7, 367–385. http://dx.doi.org/10.1109/TEVC.2003.814633.

Anparasan, A., Lejeune, M., 2019. Resource deployment and donation allocation for epidemic outbreaks. Ann. Oper. Res. 283, 9–32. http://dx.doi.org/10.1007/s10479-016-2392-0.

Araz, Ö., Galvani, A., Meyers, L., 2012. Geographic prioritization of distributing pandemic influenza vaccines. Health Care Manage. Sci. 15, 175–187. http://dx.doi.org/10.1007/s10729-012-9199-6.

Bergman, M., Viscusi, D., Zhuang, Z., Palmiero, A., Powell, J., Shaffer, R., 2012. Impact of multiple consecutive donnings on filtering facepiece respirator fit. Am. J. Infect. Control 40, 375–380. http://dx.doi.org/10.1016/j.ajic.2011.05.003.

Binkley, C., Kemp, D., 2020. Ethical rationing of personal protective equipment to minimize moral residue during the covid-19 pandemic. J. Am. Coll. Surg. 230, 1111–1113. http://dx.doi.org/10.1016/j.jamcollsurg.2020.03.031.

Brandeau, M.L., 2005. Allocating resources to control infectious diseases. In: Operations Research and Health Care. Springer, pp. 443–464, chapter 17.

Browne, S., Yechiali, U., 1989. Dynamic priority rules for cyclic-type queues. Adv. Appl. Probab. 432–450. http://dx.doi.org/10.2307/1427168.

Büyüktahtakın, I., des Bordes, E., Kıbış, E., 2018. A new epidemics–logistics model: Insights into controlling the ebola virus disease in west Africa. Eur. J. Oper. Res. 265, 1046–1063. http://dx.doi.org/10.1016/j.ejor.2017.08.037.

CDC, 2015. Hierarchy of controls. https://www.cdc.gov/niosh/topics/hierarchy/default.html. (Accessed 6 May 2021).

CDC, 2016. Transmission-based precautions. https://www.cdc.gov/infectioncontrol/basics/transmission-based-precautions.html. (Accessed 6 May 2021).

CDC, 2017. Severe acute respiratory syndrome (SARS). https://www.cdc.gov/sars/about/fs-sars.html. (Accessed 6 May 2021).

CDC, 2019a. 2009 H1N1 Pandemic (H1N1pdm09 virus). https://www.cdc.gov/flu/pandemic-resources/2009-h1n1-pandemic.html. (Accessed 6 May 2021).

CDC, 2019b. Types of respiratory protection. https://www.cdc.gov/coronavirus/2019-ncov/hcp/elastomeric-respirators-strategy/respiratory-protection.html. (Accessed 6 May 2021).

CDC, 2020a. Duration of isolation and precautions for adults with COVID-19. https://www.cdc.gov/coronavirus/2019-ncov/hcp/duration-isolation.html. (Accessed 6 May 2021).
CDC, 2020b. General optimization strategies. https://www.cdc.gov/coronavirus/2019-ncov/hcp/ppe-strategy/general-optimization-strategies.html. (Accessed 6 May 2021).
CDC, 2020c. Using personal protective equipment (PPE). https://www.cdc.gov/coronavirus/2019-ncov/hcp/using-ppe.html. (Accessed 6 May 2021).
Chen, W., Gurnet, A., Ruiz, A., 2015. Modelling the logistics response to a general infectious disease. IFAC-PapersOnLine 48, 180–186. http://dx.doi.org/10.1016/j.ifacol.2015.06.078.
Choewell, G., Sattenspiel, L., Viboud, C., 2016. Mathematical models to characterize early epidemic growth: A review. Phys. Life Rev. 18, 66–97. http://dx.doi.org/10.1016/j.plrev.2016.07.005.
Crow, J., Kimura, M., 1979. Efficiency of truncation selection. Proc. Natl. Acad. Sci. 76, 396–399. http://dx.doi.org/10.1073/pnas.76.1.396.
Dasaklis, T., Pappis, C., Rachaniotis, N., 2012. Epidemics control and logistics operations: A review. Int. J. Prod. Econ. 139, 393–410. http://dx.doi.org/10.1016/j.ijpe.2012.05.023.
Deb, K., Pratap, A., Agarwal, S., Meyarivan, T., 2002. A fast and elitist multiobjective genetic algorithm: NSGA-II. IEEE Trans. Evol. Comput. 6, 182–197. http://dx.doi.org/10.1109/4235.996017.
Duan, W., Fan, Z., Zhang, P., Guo, G., Qui, X., 2015. Mathematical and computational approaches to epidemic modeling: a comprehensive review. Front. Comput. Sci. 9, 806–826. http://dx.doi.org/10.1007/s11704-014-3369-2.
Eikenberry, S., Mancuso, M., Iboi, E., Phan, T., Eikenberry, K., Kuang, Y., Kostelich, E., Gumel, A., 2020. To mask or not to mask: Modeling the potential for face mask use by the general public to curtail the covid-19 pandemic. Infect. Dis. Model. 5, 293–308. http://dx.doi.org/10.1016/j.idm.2020.04.001.
Emanuel, E., Govind, P., Upshur, R., Thome, B., Parker, M., Glickman, A., Zhang, C., Boyle, C., Smith, M., Phillips, J., 2020. Fair allocation of scarce medical resources in the time of covid-19. N. Engl. J. Med. 382, 2049–2055. http://dx.doi.org/10.1056/NEJMsb2005114.
Enayati, S., Özaltın, O., 2020. Optimal influenza vaccine distribution with equity. Eur. J. Oper. Res. 283, 714–725. http://dx.doi.org/10.1016/j.ejor.2019.11.025.
Gamchi, N., Torabi, S., Jolai, F., 2021. A novel vehicle routing problem for vaccine distribution using sir epidemic model. OR Spectr. 9, 1–34. http://dx.doi.org/10.1007/s00291-020-00609-6.
Göçmen, E., 2020. Linear programming with fuzzy parameters for inventory routing problem in effective management of personal protective equipment: a case study of corona virus disease 2019. Energy Sources A 1–15. http://dx.doi.org/10.1080/15567036.2020.1861133.
Haimes, Y., Lasdon, L., Wismer, D., 1971. On a bicriterion formulation of the problems of integrated system identification and system optimization. IEEE Trans. Syst. Man Cybern. 1, 296–297. http://dx.doi.org/10.1109/TSMC.1971.4308298.
Hamid, N., Abounacer, R., Idali Oumhand, M., Feddaoui, M., Agliz, D., 2019. Parameters identification of photovoltaic solar cells and module using the genetic algorithm with convex combination crossover. Int. J. Ambient Energy 40, 517–524. http://dx.doi.org/10.1080/01430750.2017.1421577.
Hasançebi, O., Erbatur, F., 2000. Evaluation of crossover techniques in genetic algorithm based optimum structural design. Comput. Struct. 78, 435–448. http://dx.doi.org/10.1016/S0045-7949(00)00089-4.
Hashikura, M., Kizu, J., 2009. Stockpile of personal protective equipment in hospital settings: preparedness for influenza pandemics. Am. J. Inf. Control 37, 703–707. http://dx.doi.org/10.1016/j.ajic.2009.05.002.
Holguín-Veras, J., Pérez, N., Jaller, M., van Wassenhove, L., Aros-Vera, F., 2013. On the appropriate objective function for post-disaster humanitarian logistics models. J. Oper. Manage. 31, 262–280. http://dx.doi.org/10.1016/j.jom.2013.06.002.
International Federation of Red Cross and Red Crescent Societies, 2020. Types of disasters: Definition of hazard. https://www.ifrc.org/en/what-we-do/disaster-management/about-disasters/definition-of-hazard/. (Accessed 6 May 2021).
Jebari, K., Madiafi, M., Elmoujahid, A., 2013. Parent selection operators for genetic algorithms. Int. J. Eng. Res. Technol. 12, 1141–1145.
Kaplan, E., Pollack, H., 1998. Allocating hiv prevention resources. Soc. Econ. Plan. Sci. 32, 257–263. http://dx.doi.org/10.1016/S0038-0121(98)00002-0.
Koyuncu, M., Erol, R., 2010. Optimal resource allocation model to mitigate the impact of pandemic influenza: a case study for turkey. J. Med. Syst. 34, 61–70. http://dx.doi.org/10.1007/s10916-008-9216-y.
Lasry, A., Zaric, S., Carter, M., 2007. Multi-level resource allocation for hiv prevention: A model for developing countries. Eur. J. Oper. Res. 180, 786–799. http://dx.doi.org/10.1016/j.ejor.2006.02.043.
Lee, S., Golinski, M., Chowell, G., 2012. Modeling optimal age-specific vaccination strategies against pandemic influenza. Bull. Math. Biol. 74, 958–980. http://dx.doi.org/10.1007/s11538-011-9704-y.
Lee, E., Maheshwary, S., Mason, J., Glisson, W., 2006. Decision support system for mass dispensing of medications for infectious disease outbreaks and bioterrorist attacks. Ann. Oper. Res. 148, 25–53. http://dx.doi.org/10.1007/s10479-006-0087-7.
Lee, E., Smalley, H., Zhang, Y., Pietz, F., Benecke, B., 2009. Facility location and multi-modality mass dispensing strategies and emergency response for biodefence and infectious disease outbreaks. Int. J. Disaster Risk Reduct. 12, 311–351. http://dx.doi.org/10.1504/IJRAM.2009.025925.
Li, X., Pan, Y., Jiang, S., Huang, Q., Chen, Z., Zhang, M., Zhang, Z., 2021. Locate vaccination stations considering travel distance, operational cost, and work schedule. Omega 101, 102236. http://dx.doi.org/10.1016/j.omega.2020.102236.
Lipowski, A., Lipowska, D., 2012. Roulette-wheel selection via stochastic acceptance. Phys. A 391, 2193–2196. http://dx.doi.org/10.1016/j.physa.2011.12.004.
Liu, M., Cao, J., Liang, J., Chen, M., 2020. Epidemic-Logistics Modeling: A New Perspective on Operations Research. Springer, Singapore.
Liu, M., Liang, J., 2013. Dynamic optimization model for allocating medical resources in epidemic controlling. J. Ind. Eng. Manage. 6, 73–88. http://dx.doi.org/10.3926/jiem.663.
Liu, M., Zhang, Z., Zhang, D., 2015. A dynamic allocation model for medical resources in the control of influenza diffusion. J. Syst. Sci. Syst. Eng. 24, 276–292. http://dx.doi.org/10.1007/s11518-015-5276-y.
Long, E., Nohdurft, E., Spinler, S., 2018. Spatial resource allocation for emerging epidemics: A comparison of greedy, myopic, and dynamic policies. Manuf. Serv. Oper. Manag. 20, 181–198. http://dx.doi.org/10.1287/msom.2017.0681.
Malmir, B., Zobel, C., 2021. An applied approach to multi-criteria humanitarian supply chain planning for pandemic response. J. Humanit. Logist. Supply Chain Manage. 11, 320–346. http://dx.doi.org/10.1108/JHLSCM-08-2020-0064.
Miller, B., Goldberg, D., 1995. Genetic algorithms, tournament selection, and the effects of noise. Complex Syst. 9, 193–212.
Mitchell, M., 1996. An Introduction to Genetic Algorithms. MIT Press, Cambridge, Mass.
Murata, T., Ishibuchi, H., Tanaka, H., 1996. Multi-objective genetic algorithm and its applications to flowshop scheduling. Comput. Ind. Eng. 30, 957–968. http://dx.doi.org/10.1016/0360-8352(96)00045-9.
Nandi, A., Medal, H., 2016. Methods for removing links in a network to minimize the spread of infections. Comput. Oper. Res. 69, 10–24. http://dx.doi.org/10.1016/j.cor.2015.11.001.
Patel, A., D'Alessandro, M., Ireland, K., Burel, W., Wencil, E., Rasmussen, S., 2017. Personal protective equipment supply chain: lessons learned from recent public health emergency responses. Health Secur. 15, 244–252. http://dx.doi.org/10.1089/hs.2016.0129.
Paul, S., Venkateswaran, J., 2018. Inventory management strategies for mitigating unfolding epidemics. IISE Trans. Healthc. Syst. Eng. 8, 167–180. http://dx.doi.org/10.1080/24725579.2017.1418768.
Qu, B., Suganthan, P., 2010. Multi-objective evolutionary algorithms based on the summation of normalized objectives and diversified selection. Inf. Sci. 180, 3170–3181. http://dx.doi.org/10.1016/j.ins.2010.05.013.
Rachaniotis, N., Dasaklis, T., Pappis, C., 2017. Controlling infectious disease outbreaks: a deterministic allocation-scheduling model with multiple discrete resources. J. Syst. Sci. Syst. Eng. 26, 219–239. http://dx.doi.org/10.1007/s11518-016-5327-z.
Ren, Y., Ordóñez, F., Wu, S., 2013. Optimal resource allocation response to a smallpox outbreak. Comput. Ind. Eng. 66, 325–337. http://dx.doi.org/10.1016/j.cie.2013.07.002.
Rico, F., Salari, E., Centeno, G., 2007. Emergency departments nurse allocation to face a pandemic influenza outbreak. In: 2007 Winter Simulation Conference. IEEE, pp. 1292–1298. http://dx.doi.org/10.1109/WSC.2007.4419734.
Rowan, N., Laffey, J., 2020. Challenges and solutions for addressing critical shortage of supply chain for personal and protective equipment (PPE) arising from coronavirus disease (COVID19) pandemic–case study from the Republic of Ireland. Sci. Total Environ. 725, 138532. http://dx.doi.org/10.1016/j.scitotenv.2020.138532.
Santini, A., 2021. Optimising the assignment of swabs and reagent for pcr testing during a viral epidemic. Omega 102, 102341. http://dx.doi.org/10.1016/j.omega.2020.102341.
Shao, J., Wang, X., Liang, C., Holguín-Veras, J., 2020. Research progress on deprivation costs in humanitarian logistics. Int. J. Disaster Risk Reduct. 42, 101343. http://dx.doi.org/10.1016/j.ijdrr.2019.101343.
Shukla, A., Pandey, H.M., Mehrotra, D., 2015. Comparative review of selection techniques in genetic algorithm. In: 2015 International Conference on Futuristic Trends on Computational Analysis and Knowledge Management (ABLAZE). pp. 515–519. http://dx.doi.org/10.1109/ABLAZE.2015.7154916.
Sokat, K., Altay, N., 2021. Serving vulnerable populations under the threat of epidemics and pandemics. J. Humanit. Logist. Supply Chain Manage. 11, 176–197. http://dx.doi.org/10.1108/JHLSCM-08-2020-0070.
Sun, L., Depuy, G., Evans, G., 2014. Multi-objective optimization models for patient allocation during a pandemic influenza outbreak. Comput. Oper. Res. 51, 350–359. http://dx.doi.org/10.1016/j.cor.2013.12.001.
Sun, P., Yang, L., De Véricourt, F., 2009. Selfish drug allocation for containing an international influenza pandemic at the onset. Oper. Res. 57, 1320–1332. http://dx.doi.org/10.1287/opre.1090.0762.
Tanner, M., Ntaimo, L., 2010. IIS branch-and-cut for joint chance-constrained stochastic programs and application to optimal vaccine allocation. Eur. J. Oper. Res. 207, 290–296. http://dx.doi.org/10.1016/j.ejor.2010.04.019.
Teytelman, A., Larson, R., 2013. Multiregional dynamic vaccine allocation during an influenza epidemic. Serv. Sci. 5, 197–215. http://dx.doi.org/10.1287/serv.2013.0046.
Ting, C., Ko, C., Huang, C., 2009. Selecting survivors in genetic algorithm using tabu search strategies. Memet. Comput. 1, 191–203. http://dx.doi.org/10.1007/s12293-009-0013-z.

Tuckwell, H., Williams, R., 2007. Some properties of a simple stochastic epidemic model of SIR type. Math. Biosci. 208, 76–97. http://dx.doi.org/10.1016/j.mbs.2006.09.018.

Ventresca, M., Aleman, D., 2014. A randomized algorithm with local search for containment of pandemic disease spread. Comput. Oper. Res. 48, 11–19. http://dx.doi.org/10.1016/j.cor.2014.02.003.

While, L., Hingston, P., Barone, L., Huband, S., 2006. A faster algorithm for calculating hypervolume. IEEE Trans. Evol. Comput. 10, 29–38. http://dx.doi.org/10.1109/TEVC.2005.851275.

WHO, 2013. Aerosol generating procedures. https://www.hse.ie/eng/about/who/healthwellbeing/infectcont/sth/resources/aerosol-generating-procedures.pdf. (Accessed 6 May 2021).

WHO, 2017. Pandemic influenza risk management. https://www.who.int/influenza/preparedness/pandemic/influenza_risk_management/en/. (Accessed 6 May 2021).

WHO, 2020a. Rational use of personal protective equipment for coronavirus disease 2019 (COVID-19). https://apps.who.int/iris/bitstream/handle/10665/331215/WHO-2019-nCov-IPCPPE_use-2020.1-eng.pdf. (Accessed 6 May 2021).

WHO, 2020b. Shortage of personal protective equipment endangering health workers worldwide. https://www.who.int/news/item/03-03-2020-shortage-of-personal-protective-equipment-endangering-health-workers-worldwide. (Accessed 6 May 2021).

WHO, 2020c. WHO coronavirus disease (COVID-19) dashboard. https://covid19.who.int/. (Accessed 6 May 2021).

Wu, J., Leung, K., Leung, G., 2020. Nowcasting and forecasting the potential domestic and international spread of the 2019-ncov outbreak originating in Wuhan, China: a modelling study. Lancet 395, 689–697. http://dx.doi.org/10.1016/S0140-6736(20)30260-9.

Yang, Y., Bidkhori, H., Rajgopal, J., 2021. Optimizing vaccine distribution networks in low and middle-income countries. Omega 99, 102197. http://dx.doi.org/10.1016/j.omega.2020.102197.

Yarmand, H., Ivy, J., Denton, B., Lloyd, A., 2014. Optimal two-phase vaccine allocation to geographically different regions under uncertainty. Eur. J. Oper. Res. 233, 208–219. http://dx.doi.org/10.1016/j.ejor.2013.08.027.

Yin, X., Büyüktahtakın, I., 2021. A multi-stage stochastic programming approach to epidemic resource allocation with equity considerations. Health Care Manage. Sci. 1–58. http://dx.doi.org/10.2139/ssrn.3792473.

Zaric, G., Brandeau, M., 2002. Dynamic resource allocation for epidemic control in multiple populations. Math. Med. Biol. 19, 235–255. http://dx.doi.org/10.1093/imammb/19.4.235.

Zhu, J., Lee, S., Wang, D., Lee, H., 2014. Effects of long-duration wearing of n95 respirator and surgical facemask: a pilot study. J. Lung Pulm Respir. Res. 1, 97–100. http://dx.doi.org/10.15406/jlprr.2014.01.00021.

Zitzler, E., 1999. Evolutionary Algorithms for Multiobjective Optimization: Methods and Applications (Dissertation). Swiss Federal Institute of Technology.